References

Agami R, Blandino G, Oren M, Shaul Y. (1999). *Nature* **399**: 809–813.
Balint E, Bates S, Vousden KH. (1999). *Oncogene* **18**: 3923–3929.
Bayon Y, Ortiz MA, Lopez-hernandez FJ, Gao F, Karin M, Pfahl M *et al.* (2003). *Mol Cell Biol* **23**: 1061–1074.
Beg AA, Baltimore D. (1996). *Science* **274**: 782–784.
Beg AA, Sha WC, Bronson RT, Baltimore D. (1995). *Nature* **376**: 167–170.
Bernassola F, Salomoni P, Oberst A, Di Como CJ, Pagano M, Melino G *et al.* (2004). *J Exp Med* **199**: 1545–1557.
Bourdon JC, Fernandes K, Murray-Zmijewski F, Liu G, Diot A, Xirodimas DP *et al.* (2005). *Genes Dev* **19**: 2122–2137.
Chang L, Kamata H, Solinas G, Luo JL, Maeda S, Venuprasad K *et al.* (2006). *Cell* **124**: 601–613.
Flores ER, Tsai KY, Crowley D, Sengupta S, Yang A, McKeon F *et al.* (2002). *Nature* **416**: 560–564.
Fontemaggi G, Gurtner A, Strano S, Higashi Y, Sacchi A, Piaggio G *et al.* (2001). *Mol Cell Biol* **21**: 8461–8470.
Gong J, Costanzo A, Yang HQ, Melino G, Kaelin Jr WG, Levrero M *et al.* (1999). *Nature* **399**: 806–809.
Gressner O, Schilling T, Lorenz K, Schulze Schleithoff E, Koch A, Schulze-Bergkamen H *et al.* (2005). *EMBO J* **24**: 2458–2471.
Grob TJ, Novak U, Maisse C, Barcaroli D, Luthi AU, Pirnia F *et al.* (2001). *Cell Death Differ* **8**: 1213–1223.
Huang TT, Wuerzberger-Davis SM, Seufzer BJ, Shumway SD, Kurama T, Boothman DA *et al.* (2000). *J Biol Chem* **275**: 9501–9509.
Ikawa S, Nakagawara A, Ikawa Y. (1999). *Cell Death Differ* **6**: 1154–1161.
Irwin MS, Kondo K, Marin MC, Cheng LS, Hahn WC, Kaelin Jr WG. (2003). *Cancer Cell* **3**: 403–410.
Jost CA, Marin MC, Kaelin Jr WG. (1997). *Nature* **389**: 191–194.
Kaghad M, Bonnet H, Yang A, Creancier L, Biscan JC, Valent A *et al.* (1997). *Cell* **90**: 809–819.
Kawai H, Nie L, Yuan ZM. (2002). *Mol Cell Biol* **22**: 6079–6088.
Kharbanda S, Ren R, Pandey P, Shafman TD, Feller SM, Weichselbaum RR *et al.* (1995). *Nature* **376**: 785–788.
Kim JS, Lee JM, Chwae YJ, Kim YH, Lee JH, Kim K *et al.* (2004). *Biochem Pharmacol* **67**: 1459–1468.
Kramer S, Ozaki T, Miyazaki K, Kato C, Hanamoto T, Nakagawara A. (2005). *Oncogene* **24**: 938–944.
Lee CW, La Thangue NB. (1999). *Oncogene* **18**: 4171–4181.
Leng RP, Lin Y, Ma W, Wu H, Lemmers B, Chung S *et al.* (2003). *Cell* **112**: 779–791.
Lissy NA, Davis PK, Irwin M, Kaelin Jr WG, Dowdy SF. (2000). *Nature* **407**: 642–645.
Mantovani F, Piazza S, Gostissa M, Strano S, Zacchi P, Mantovani R *et al.* (2004). *Mol Cell* **14**: 625–636.
Melino G, De Laurenzi V, Vousden KH. (2002). *Nat Rev Cancer* **2**: 605–615.
Muta T, Takeshige K. (2001). *Eur J Biochem* **268**: 4580–4589.
Nakagawa T, Takahashi M, Ozaki T, Watanabe K, Todo S, Mizuguchi H *et al.* (2002). *Mol Cell Biol* **22**: 2575–2585.
Pozniak CD, Radinovic S, Yang A, McKeon F, Kaplan DR, Miller FD. (2000). *Science* **289**: 304–306.
Rossi M, De Laurenzi V, Munarriz E, Green DR, Liu YC, Vousden KH *et al.* (2005). *EMBO J* **24**: 836–848.
Stiewe T, Putzer BM. (2002). *Cell Death Differ* **9**: 237–245.
Stiewe T, Zimmermann S, Frilling A, Esche H, Putzer BM. (2002). *Cancer Res* **62**: 3598–3602.
Strano S, Monti O, Pediconi N, Baccarini A, Fontemaggi G, Lapi E *et al.* (2005). *Mol Cell* **18**: 447–459.
Van Antwerp DJ, Martin SJ, Kafri T, Green DR, Verma IM. (1996). *Science* **274**: 787–789.
Wan YY, DeGregori J. (2003). *Immunity* **18**: 331–342.
Wang CY, Mayo MW, Baldwin ASJ. (1996). *Science* **274**: 784–787.
Wang CY, Mayo MW, Korneluk RG, Goeddel DV, Baldwin SJ. (1998). *Science* **281**: 1680–1683.
Yamagishi N, Miyakoshi J, Takebe H. (1997). *Int J Radiat Biol* **72**: 157–162.
Yang A, Kaghad M, Wang Y, Gillett E, Fleming MD, Dotsch V *et al.* (1998). *Mol Cell* **2**: 305–316.
Yang A, McKeon F. (2000). *Nat Rev Mol Cell Biol* **1**: 199–207.
Yang A, Walker N, Bronson R, Kaghad M, Oosterwegel M, Bonnin J *et al.* (2000). *Nature* **404**: 99–103.
Yuan ZM, Shioya H, Ishiko T, Sun X, Gu J, Huang YY *et al.* (1999). *Nature* **399**: 814–817.
Zaika AI, Slade N, Erster SH, Sansome C, Joseph TW, Pearl M *et al.* (2002). *J Exp Med* **196**: 765–780.
Zeng X, Chen L, Jost CA, Maya R, Keller D, Wang X *et al.* (1999). *Mol Cell Biol* **19**: 3257–3266.

Supplementary Information accompanies the paper on the Oncogene website (http://www.nature.com/onc).

Available online at www.sciencedirect.com
ScienceDirect
Biochemical and Biophysical Research Communications 351 (2006) 306–311
BBRC
www.elsevier.com/locate/ybbrc

Hypoxia-inducible factor-1 mediates the expression of DNA polymerase ι in human tumor cells

Akiko Ito [a,b], Nobuko Koshikawa [a], Shigenobu Mochizuki [c], Ken Omura [b], Keizo Takenaga [a,*]

[a] *Division of Chemotherapy, Chiba Cancer Center Research Institute, 666-2 Nitona, Chuoh-ku, Chiba 260-8717, Japan*
[b] *Oral and Maxillofacial Surgery, Department of Oral Restitution, Division of Oral Health Sciences, Graduate School, Tokyo Medical and Dental University, 1-5-45 Yushima, Bunkyo-ku, Tokyo 113-8549, Japan*
[c] *Division of Biochemistry, Chiba Cancer Center Research Institute, 666-2 Nitona, Chuoh-ku, Chiba 260-8717, Japan*

Received 6 October 2006
Available online 16 October 2006

Abstract

Hypoxia generated in tumors has been shown to contribute to mutations and genetic instability. However, the molecular mechanisms remain incompletely defined. Since reactive oxygen species (ROS) are overproduced immediately after reoxygenation of hypoxic cells and generate oxidized guanine, we assumed that the mechanisms might involve translesion DNA polymerases that can bypass oxidized guanine. We report here that hypoxia as well as hypoxia mimetics, desferrioxamine, and $CoCl_2$, enhanced the expression of DNA polymerase ι (pol ι) in human tumor cell lines. Searching the consensus sequence of hypoxia response element to which HIF-1 binds revealed that it locates in the intron 1 of the *pol ι* gene. These results suggest that HIF-1-mediated *pol ι* gene expression may be involved in the generation of translesion mutations during DNA replication after hypoxia followed by reoxygenation, thereby contributing to the accumulation of genetic changes in tumor cells.

Keywords: Hypoxia; HIF-1; Translesion DNA polymerase; DNA polymerase ι; Reactive oxygen species; 8-Oxoguanine

Tumor cells under hypoxic conditions activate many genes including those related to cell survival, glycolysis, and angiogenesis [1,2]. The oxygen sensing mechanisms have been extensively studied and revealed to involve hypoxia-inducible factors (HIFs) as key regulatory transcription factors that are composed of HIF-α subunit and HIF-β/ARNT subunit [1,2]. Under normoxic conditions, the α subunit of HIF-1 (HIF-1α) is hydroxylated at proline-564 and proline-402 residues by specific Fe^{2+}, oxoglutarate, and oxygen-dependent hydroxylases, recognized and ubiquitinated by an E3 ubiquitin ligase complex consisting of the tumor suppressor VHL (von Hippel–Lindau), elongin B and elongin C, and rapidly degraded through the ubiquitin-proteasome pathway while the β subunit of HIF-1 (HIF-1β) is constitutively expressed [3]. Under hypoxic conditions, HIF-1α is stabilized, allowing its nuclear translocation and dimerization with HIF-1β [4]. Chelating or substituting Fe^{2+} with desferrioxamine or $CoCl_2$, respectively, reduces the hydroxylase activity and mimics hypoxia [5,6]. In the nucleus, HIF-1 binds to the hypoxia response element (HRE) of hypoxia-inducible genes and transactivates their transcription. The consensus sequence of HRE has been shown to be 5′-(A/G)CGTG-3′ [7].

It has been shown that exposure of cells to hypoxia results in increased frequencies of point mutations such as C:G → A:T and T:A → G:C transversions [8]. Although the mechanisms underlying hypoxia-induced mutagenesis are not well understood, reactive oxygen species (ROS) are inevitably involved in the mechanisms because ROS are overproduced during reoxygenation and generate

* Corresponding author. Fax: +81 43 265 4459.
E-mail address: keizo@chiba-cc.jp (K. Takenaga).

0006-291X/$ - see front matter © 2006 Elsevier Inc. All rights reserved.
doi:10.1016/j.bbrc.2006.10.048

highly mutagenic base 8-hydroxyguanine (8-oxo-dG) [9]. The presence of 8-oxo-dG in DNA causes C:G → A:T and T:A → G:C transversions in DNA, since, unless repaired, 8-oxo-dG allows the misincorporation of cytosine and adenine nucleotides opposite the lesion during DNA replication [10].

Recently, several studies suggest the involvement of the deregulation of DNA repair pathways in hypoxia-induced mutagenesis [8,11,12]. Mihaylova et al. reported decreased expression of the DNA mismatch repair gene *Mlh1* under hypoxic conditions [11]. Koshiji et al. demonstrated that HIF-1 induces genetic instability by transcriptionally down-regulating the expression of MutSα which recognizes base mismatches [12]. Hypoxia may cause mutagenesis, at least in part, by hindering repair of ROS-induced DNA damage through down-regulation of DNA mismatch repair enzymes.

To date, several DNA polymerases that are clearly involved in translesion synthesis including Pol η (RAD30), Pol ι (RAD30B), Pol θ, Pol κ, and Rev1 which belong to the Y superfamily have been reported [13]. One of their most distinct features is a high error propensity during DNA synthesis. Among these Y family polymerases, Pol η, Pol ι, and Pol κ can efficiently bypass 8-oxo-dG [14–16]. Pol μ which belongs to the X superfamily has also been reported to possess efficient lesion bypass activities in response to several types of DNA damage including 8-oxo-dG [17].

We hypothesized that translesion DNA polymerases that can bypass 8-oxo-dG might be involved in the generation of mutations after hypoxia/reoxygenation. We report here that hypoxia enhances the expression of *pol ι* gene through HIF-1 interaction with the consensus HRE site in the intron 1 of the gene.

Materials and methods

Cells and cell culture. Human cervical carcinoma HeLa cells, hepatocarcinoma HepG2 cells, mammary carcinoma MCF-7 and MDA-MB-231 cells, lung adenocarcinoma A549 cells, fibrosarcoma HT1080 cells, colon carcinoma LS174T cells, and glioma U87MG cells were cultured at 37 °C in a humidified atmosphere with 21% O_2/5% CO_2 (normoxia) or 1% O_2/5% CO_2 (hypoxia).

Detection of ROS generation. ROS generation was detected with 2′,7′-dichlorofluorescin diacetate (DCFH-DA) (Molecular Probe, Inc., Eugene, OR) as described previously [18].

Immunostaining of 8-oxo-dG. HeLa cells on glass coverslips were cultured in 21% O_2, or 1% O_2 for 24 h, or 1% O_2 for 24 h followed by 21% O_2 for 30 min. Staining for 8-oxo-dG with anti-8-oxo-dG antibody 1F7 (Trevigen, Inc., Gaithersburg, MD) was performed according to the manufacturer's instructions with some modifications. Briefly, the cells fixed with 70% ethanol at −20 °C were treated with RNase (100 μg/ml) in 10 mM Tris–HCl, pH 7.5, and 1 mM EDTA, and 0.4 M NaCl for 1 h at 37 °C. DNA was denatured with 4 N HCl for 7 min at room temperature. After neutralization, the cells were incubated with 10% fetal bovine serum, and then incubated with anti-8-oxo-dG antibody at 4 °C overnight followed by TRITC-conjugated goat anti-mouse IgG. The nuclei were stained with DAPI (1 μg/ml).

SDS–PAGE and Western blotting. Total cell lysates were prepared by directly solubilizing cells in SDS sample buffer. Nuclear extracts were prepared by using Nuclear Extract Kit (Active Motif, Carlsbad, CA). Proteins were resolved by SDS–PAGE and transferred to nitrocellulose membrane. The membrane was incubated with mouse anti-HIF-1α (Novus Biologicals, Littleton, NO), goat anti-pol ι antibody (Santa Cruz Biotechnology, Inc., Santa Cruz, CA) or rabbit anti-E2F-1 antibody (Santa Cruz Biotechnology) followed by incubation with appropriate horseradish peroxidase-conjugated secondary antibody. Proteins were detected using ECL Western blotting detection reagents (Amersham Biosciences, Buckinghamshire, UK).

Semi-quantitative RT-PCR. One microgram of total RNA, which was extracted with guanidinium thiocyanate, was reverse transcribed into cDNA, and the resulting cDNA was used for amplification of target cDNAs using *rTaq* DNA polymerase (TOYOBO, Osaka). The sense and antisense oligonucleotide primers used for PCR were: 5′-GCTGTG CTGGAGTGGCTTCT-3′ and 5′-GCCAGAGCGTGAAGTAGTTG-3′ for *pol ι*, 5′-GCCATGCCAGGATTTATTGCTA-3′ and 5′-CTCCTTTG TTGGTGTTTCCT-3′ for *pol κ*, 5′-ACCCAGGCAACTACCCAAAAC-3′ and 5′-GGGCTCAGTTCCTGTACTTTG-3′ for *pol η*, 5′-AGCCTG-TACCTGTGGAGTGC-3′ and 5′-CCAGGCGGGTAGGGGACTCA-3′ for *pol μ*, 5′-ATGCCTCAACCGTGGACAAT-3′ and 5′-CTTGCT CTCGATGTGCTGC-3′ for *Mlh1*, 5′-GCAGAATCATCACGAA GTGG-3′ and 5′-GCATGGTGATGTTGGACTCC-3′ for *VEGF*, and 5′-TGACGGGGTGACCCACACTGTGCCCATCTA-3′ and 5′-CTAGAA GCATTTGCGGTGGACGATGGAGGG-3′ for *β-actin*, respectively. The PCR conditions were: 95 °C for 2 min, and then 30 cycles with 95 °C for 10 s, 59 °C for 10 s, 72 °C for 1 min for *pol ι*, *pol η*, and *VEGF*, 30 cycles with 95 °C for 5 s, 61 °C for 10 s, 72 °C for 2 min for *pol κ*, 30 cycles with 95 °C for 5 s, 65 °C for 10 s, 72 °C for 1.5 min for *pol μ*, 30 cycles with 95 °C for 5 s, 59 °C for 10 s, 72 °C for 1 min for *Mlh1* or 25 cycles with 95 °C for 5 s, 59 °C for 10 s, 72 °C for 1 min for *β-actin*, and 72 °C for 5 min.

Construction of plasmids. The plasmid pcDNA3.1/HIF-1α^{DN} expressing dominant-negative HIF-1α was prepared essentially as described previously [19]. The plasmid expressing constitutively active HIF-1α, pcDNA3.1/HIF-1α$^{P402A/P564A}$, was constructed by introducing mutations into pcDNA3.1/HIF-1α that change both proline-402 and proline-564 of HIF-1α to alanine by using QuikChange® Site Directed Mutagenesis Kit (Stratagene, La Jolla, CA). A luciferase reporter plasmid harboring the regulatory region (from −1346 to +418) of human *pol ι* gene, where +1 represents the transcription start site, was constructed as follows. First, a DNA fragment was amplified by PCR using genomic DNA, the 5′-primer carrying *Kpn*I site at the 5′ end, 5′-GGTACCCCTCCCTTCTGTCTG TGGA-3′, and the 3′ primer carrying *Sac*I site at the 5′ end, 5′-GAG CTCCTCGGCGTCTTCCTCGTCG-3′, and *Ex Taq*® DNA polymerase (TaKaRa Bio, Shiga). The resulting PCR product was subcloned into pGEM-T Easy vector (Promega Corp., Madison, WI), generating a plasmid pGEM/pol ι. After digesting with *Kpn*I and *Sac*I, the insert was ligated into the *Kpn*I/*Sac*I-cut pGL2-basic (Promega), generating a pGL2/pol ι reporter plasmid. Introduction of a mutation into the core sequence of putative HREs of *pol ι* (named HRE1 (from −400 to −396, 5′-GCGTG-3′), HRE2 (from −176 to −172, 5′-ACGTG-3′), HRE3 (from −149 to −145, 5′-GCGTG-3′), and HRE4 (from +330 to +334, 5′-ACGTG-3′)) that changes the sequence 5′-(A/G)CGTG-3′ to 5′-(A/G)AAAG-3′ was done by using QuikChange® Site Directed Mutagenesis Kit and pGEM/pol ι as a template. The identity of all of the cloned fragments was verified by nucleotide sequence analysis.

Luciferase reporter assays. Transient transfection of the luciferase reporter constructs into HepG2 cells and luciferase reporter assays were carried out as described previously [18]. One day after transfection, the cells were exposed to hypoxia (1% O_2) for 18 h, and luciferase activities in cell extracts were measured.

Electrophoretic mobility shift assay (EMSA). The nuclear proteins for EMSA were prepared from HeLa cells cultured in 21% O_2 or 1% O_2 for 8 h as described previously [20]. The HRE4-specific double-stranded oligonucleotide probe (wtHRE4) or its mutant form (mutHRE4) was prepared by annealing the sense 5′-ACTACAAATACGTGTCGAGGGT-3′ and the antisense 5′-ACCCTCGACACGTATTTGTAGT-3′ oligonucleotides (from +321 to +341) (containing putative HRE (marked in bold type)) or the sense 5′-ACTACAAATAAAAGTCGAGGGT-3′ and the

antisense 5′-ACCCTCGACTTTTATTTGTAGT-3′ oligonucleotides (containing mutated HRE (underlined)), respectively. Ten micrograms of nuclear proteins, ^{32}P-labeled double-stranded probe, 0.4 μg of calf thymus DNA, and binding buffer (10 mM Tris–HCl, pH 7.5, 50 mM NaCl, 1 mM $MgCl_2$, 1 mM EDTA, 5% glycerol, and 5 mM DTT) were mixed in a total volume of 20 μl. In competition assays, 40-fold molar excess amount of unlabeled competitors was included in the reaction mixture. The mixture was incubated at room temperature for 30 min and then loaded on a 4% polyacrylamide gel in TBE buffer (89 mM Tris base, 89 mM boric acid, and 5 mM EDTA). Supershift assay was performed using 1 μg of mouse monoclonal anti-HIF-1α antibody (clone H1alpha67, Novus Biologicals) or rabbit polyclonal anti-HIF-2α antibody (Novus Biologicals).

Chromatin immunoprecipitation (ChIP) assay. HeLa cells cultured in 21% O_2 or 1% O_2 for 8 h were fixed with 1% formaldehyde for 10 min at room temperature. Preparation of chromatin solution was performed essentially as described previously [21]. The chromatin solution was incubated with 5 μg of mouse monoclonal anti-HIF-1α antibody (clone H1alpha67, Novus Biologicals) at 4 °C for 15 h. Normal mouse IgG served as a control. Immunoprecipitation, washing, and elution of immune complexes were carried out with Protein A agarose beads (Upstate, Lake Placid, NY) according to the manufacturer's protocols. After reversing cross-links, the DNA was recovered by phenol:chloroform extraction and precipitated by ethanol. The association of HIF-1α with HRE4 was examined by hot-start PCR using *GoTaq* DNA polymerase (Promega). The sense and the antisense primers used were 5′-GCTGCCTCCCTCTGCCTT-3′ (from +236 to +253) and 5′-GGTTCTGAGCCATCCCTTC-3′ (from +506 to +524), respectively.

Results

To examine whether exposure of cells to hypoxia followed by reoxygenation causes ROS overproduction, HeLa cells were cultured under hypoxic conditions for 24 h and then reoxygenated for 30 min. ROS production was detected with DCFH-DA. The results showed that some of the cells produced ROS under both normoxic and hypoxic conditions (see Supplementary data, S1a). However, at 30 min after reoxygenation, many cells were found to produce a large amount of ROS (S1a). This ROS production was transient and attenuated to the normoxic level within 2 h after reoxygenation (data not shown). Then we examined the formation of 8-oxo-dG by immunostaining the cells with anti-8-oxo-dG antibody. As expected, a larger amount of 8-oxo-dG was formed in the reoxygenated cells than in normoxic and hypoxic cells (S1b).

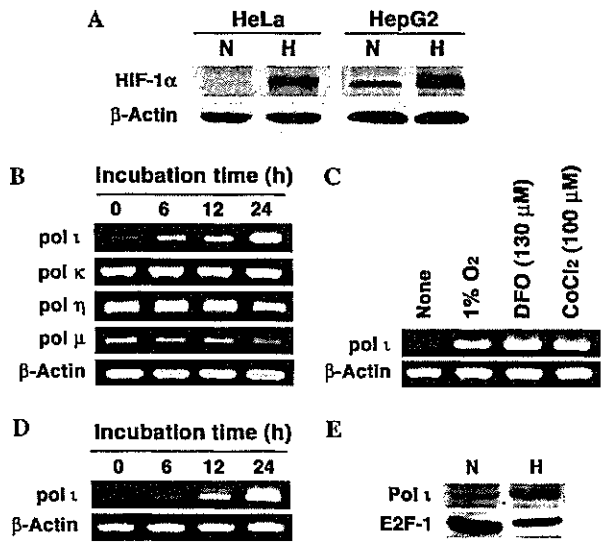

Fig. 1. Effects of hypoxia on the expressions of various error-prone DNA polymerase genes. (A) HIF-1α expression. HeLa and HepG2 cells were exposed to 1% O_2 for 6 h. Total cell lysates were subjected to immunoblot analysis. (B) Expression of mRNAs for various translesion DNA polymerases in HeLa cells exposed to 1% O_2 for the indicated times. Total RNA was subjected to RT-PCR. (C) Expression of *pol ι* mRNA in HeLa cells exposed to 1% O_2 or treated with desferrioxamine (DFO) or $CoCl_2$ for 24 h. (D) Expression of *pol ι* mRNA in HepG2 cells exposed to 1% O_2 for the indicated times. (E) Pol ι protein expression in HepG2 cells exposed to 1% O_2 for 24 h. Nuclear extracts were subjected to immunoblot analysis. E2F-1 was used as a control.

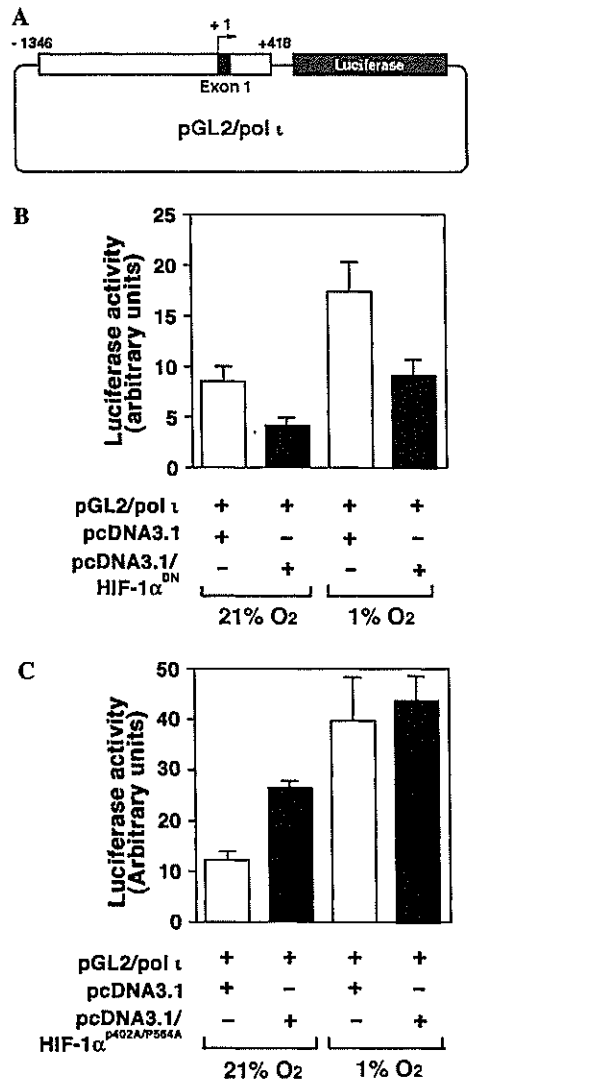

Fig. 2. Responsiveness of the luciferase reporter plasmid harboring *pol ι* regulatory region to hypoxia. (A) Construct of pGL2/pol ι luciferase reporter plasmid. (B) Effects of hypoxia and dominant-negative HIF-1α on luciferase activity. The reporter plasmid pGL2/pol ι was co-transfected with pcDNA3.1 or pcDNA3.1/HIF-1α^{DN} into HepG2 cells. The cells were exposed to 1% O_2 for 18 h. (C) Effects of hypoxia and constitutively active HIF-1α on luciferase activity. The reporter plasmid pGL2/pol ι was co-transfected with pcDNA3.1 or pcDNA3.1/HIF-1α$^{P402A/P564A}$ into HepG2 cells. Bars, SD.

Exposure of HeLa and HepG2 cells to hypoxia for 6 h resulted in the accumulation of HIF-1α (Fig. 1A). We then examined the expressions of translesion DNA polymerases that can bypass 8-oxo-dG in hypoxic cells by semi-quantitative RT-PCR. The results clearly showed that the expression of *pol ι* mRNA, but not of *pol κ*, *pol η*, or *pol μ* mRNA, was significantly increased by hypoxic stress in HeLa and HepG2 cells, depending on the incubation periods (6–24 h) (Fig. 1B and D). The hypoxia mimetics, desferrioxamine and $CoCl_2$, also increased the expression of *pol ι* mRNA (Fig. 1C). Accordingly, the amount of Pol ι protein was elevated in the nuclear extracts of HepG2 cells (Fig. 1E). Furthermore, hypoxia increased the level of *pol ι* mRNA in other cell lines such as A549, HT1080, LS174T, MCF7, MDA-MB-231, and U87MG (S2a). The induction of *pol ι* mRNA by hypoxia was observed in parallel with that of *VEGF* mRNA that is a well-known hypoxia-inducible gene. On the other hand, the decrease in the expression of *Mlh1* mRNA was detectable in both HeLa and HepG2 cells after a 48-h incubation under hypoxic conditions (S2b).

To examine whether HIF mediates the expression of *pol ι* mRNA in hypoxia, we made a pGL2/pol ι luciferase reporter construct harboring *pol ι* gene regulatory region (from −1346 to +418) (Fig. 2A). Transfection of the construct into HepG2 cells followed by exposure to hypoxia resulted in an approximately 2- to 3-fold increase in the luciferase activity (Fig. 2B and C). Co-transfection of pcDNA3.1/HIF-1α^{DN} abolished the increase (Fig. 2B). On the other hand, co-transfection with pcDNA3.1/HIF-1α$^{P402A/P564A}$ increased luciferase activity even under normoxic conditions (Fig. 2C), suggesting the involvement of HIF in the expression of *pol ι* mRNA in hypoxia.

Searching HRE consensus sequence (5′-(A/G)CGTG-3′) within this region showed that there are four putative HREs, three of them locating upstream of the transcription start site, named HRE1, HRE2, and HRE3, and the one locating in the intron 1, named HRE4. To determine which is functional, we generated a series of luciferase reporter plasmids in which three or all of the putative HREs were destroyed by introducing mutations (Fig. 3). Co-transfection of each of them with pcDNA3.1/HIF-1α$^{P402A/P564A}$ into HepG2 cells revealed that the reporter plasmid with intact HRE4 was most responsive while that with intact

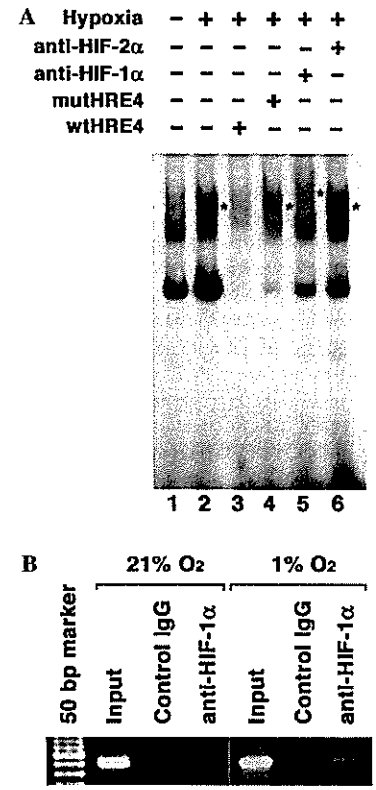

Fig. 4. HIF-1 binds to the HRE located in the intron 1 of the *pol ι* gene. (A) EMSA. Hela cells were cultured under 21% O_2 or 1% O_2 for 8 h. Nuclear extracts were subjected to EMSA using ^{32}P-labeled wtHRE4 as a probe. Asterisks indicate binding activity. (B) ChIP assay. HeLa cells were cultured under 21% O_2 or 1% O_2 for 8 h. ChIP assay was performed with mouse monoclonal anti-HIF-1α antibodies or mouse IgG as a control.

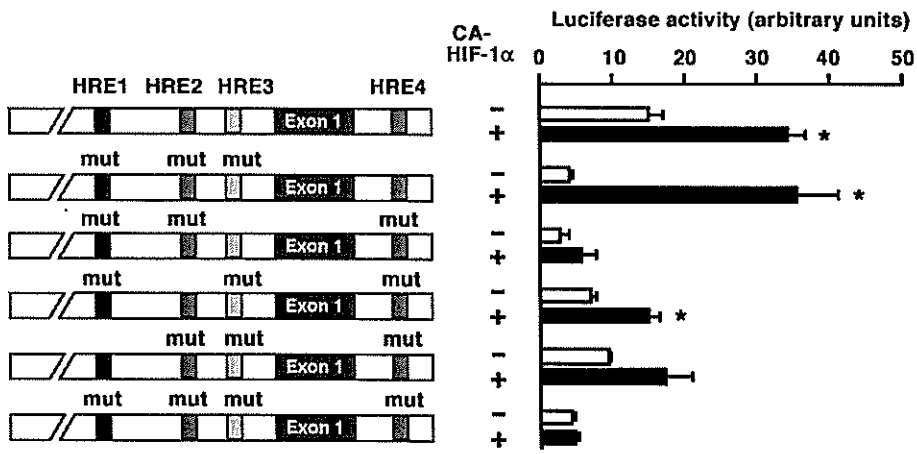

Fig. 3. Analysis of functional HRE in the *pol ι* regulatory region by luciferase reporter assays. Each of pGL2/pol ι plasmids with or without mutated (mut) HREs as indicated was co-transfected with pcDNA3.1 or pcDNA3.1/HIF-1α$^{P402A/P564A}$ (CA-HIF-1α) into HepG2 cells. The cells were exposed to 1% O_2 for 18 h. Bars, SD. *$p < 0.01$.

HRE1, HRE2, or HRE3 and that without all of the putative HREs showed weak and no responsiveness, respectively. To obtain evidence that HIF-1 binds to HRE4, we carried out EMSA using wtHRE4 as a DNA probe. The results showed that hypoxia enhanced binding activity (Fig. 4A, lane 2) that was competed with excess wtHRE4 (lane 3), but not with its mutant form mutHRE4 (lane 4). Addition of antibodies directed against HIF-1α, but not HIF-2α, induced a supershift of the binding activity (lanes 5 and 6). Furthermore, ChIP assay demonstrated that HIF-1α bound to the region containing HRE4 (Fig. 4B). From these results, we concluded that HIF-1 indeed interacts with the consensus HRE site (from +330 to +334) in the intron 1 of the *pol ι* gene.

Discussion

In this study, we confirmed that ROS were transiently overproduced in HeLa cells during reoxygenation and indeed caused 8-oxo-dG formation in the cells. We then focused on the expressions of translesion DNA polymerases that can bypass 8-oxo-dG, and found that hypoxia enhanced the expression of *pol ι* mRNA in various tumor cell lines.

Human Pol ι has low processivity and lacks an intrinsic 3′–5′ exonuclease activity, and has the lowest fidelity among so far reported eukaryotic polymerases [22]. Purified Pol ι has been observed to be able to efficiently bypass oxidized guanine and cytosine residues, as well as a variety of uracil lesions [23]. Not only can Pol ι mediate translesion replication in damaged DNA, but it also can misincorporate bases in a template-dependent manner in undamaged DNA [24,25]. Although these data are based on the *in vitro* studies, Yang et al. recently reported that Pol ι is overexpressed in human breast carcinoma cells and, importantly, that the expression level of Pol ι correlates with a significant decrease in DNA replication fidelity [26]. Therefore, up-regulation of Pol ι under hypoxic conditions might contribute to hypoxia/reoxygenation-induced mutagenesis.

Three lines of evidence suggested the involvement of HIF-1 in the mechanisms by which hypoxia induces *pol ι* mRNA expression. First, desferrioxamine and $CoCl_2$ also increased the expression of *pol ι* mRNA. Second, the reporter assays showed that dominant-negative HIF-1α suppressed the hypoxia-enhanced luciferase activity. Third, constitutively active HIF-1α enhanced the luciferase activity under normoxic conditions. Sequence analysis revealed the presence of four putative HREs which could explain the described effect of hypoxia on the induction of *pol ι* mRNA. Introduction of mutations in these HREs revealed that the reporter construct with intact HRE present in the intron 1 showed the maximal response to the co-transfected constitutively active HIF-1α construct, pointing out the major contribution of this HRE. Binding of HIF-1 to the HRE sequence was corroborated by EMSA. A shifted band was detected in hypoxic nuclear extracts, and a supershifted band was also detected after the incubation of the probe with anti-HIF-1α antibody. Since anti-HIF-2α antibody did not induce a supershifted band, HIF-2 is unlikely to bind the HRE. HIF-1 binding to the same sequence was further strengthened by the results of ChIP assay. Altogether, these results demonstrate that *pol ι* is a hypoxia-inducible gene through HIF-1 interaction with the consensus HRE site located at +330 in the intron 1 of the gene.

Recent studies highlight the deregulation of DNA mismatch repair enzymes in hypoxia as a mechanism of hypoxia-induced mutagenesis [11,12]. Loss of DNA mismatch repair renders cells hypersensitive to the mutagenic effect of oxidative stress [27]. In addition to this mechanism, our results may provide another mechanism underlying hypoxia/reoxygenation-induced mutagenesis. Through these mechanisms, hypoxia could lead to the genetic instability in tumor tissues.

Acknowledgments

This work was supported by Grants-in-Aid from the Ministry of Health, Labour, and Welfare for Third Term Comprehensive Control Research for Cancer and from the Ministry of Education, Culture, Sports, Science and Technology for Scientific Research, Japan.

Appendix A. Supplementary data

Supplementary data associated with this article can be found, in the online version, at doi:10.1016/j.bbrc.2006.10.048.

References

[1] A.L. Harris, Hypoxia—a key regulatory factor in tumour growth, Nat. Rev. Cancer 2 (2002) 38–47.
[2] G.L. Semenza, HIF-1 and tumor progression: pathophysiology and therapeutics, Trends Mol. Med. 8 (2002) S62–S67.
[3] L.E. Huang, J. Gu, M. Schau, H.F. Bunn, Regulation of hypoxia-inducible factor 1α is mediated by an O_2-dependent degradation domain via the ubiquitin-proteasome pathway, Proc. Natl. Acad. Sci. USA 95 (1998) 7987–7992.
[4] B.H. Jiang, G.L. Semenza, C. Bauer, H.H. Marti, Hypoxia-inducible factor 1 levels vary exponentially over a physiologically relevant range of O_2 tension, Am. J. Physiol. 271 (1996) C1172–C1180.
[5] G.L. Wang, G.L. Semenza, Desferrioxamine induces erythropoietin gene expression and hypoxia-inducible factor 1 DNA-binding activity: implications for models of hypoxia signal transduction, Blood 82 (1993) 3610–3615.
[6] B.L. Ebert, H.F. Bunn, Regulation of the erythropoietin gene, Blood 94 (1999) 1864–1877.
[7] G.L. Semenza, B.H. Jiang, S.W. Leung, R. Passantino, J.P. Concordet, P. Maire, A. Giallongo, Hypoxia response elements in the aldolase A, enolase 1, and lactate dehydrogenase A gene promoters contain essential binding sites for hypoxia-inducible factor 1, J. Biol. Chem. 271 (1996) 32529–32537.
[8] J. Yuan, L. Narayanan, S. Rockwell, P.M. Glazer, Diminished DNA repair and elevated mutagenesis in mammalian cells exposed to hypoxia and low pH, Cancer Res. 60 (2000) 4372–4376.
[9] A.P. Breen, J.A. Murphy, Reactions of oxyl radicals with DNA, Free Radic. Biol. Med. 18 (1995) 1033–1077.
[10] S. Shibutani, M. Takeshita, A.P. Grollman, Insertion of specific bases during DNA synthesis past the oxidation-damaged base 8-oxodG, Nature 349 (1991) 431–434.

[11] V.T. Mihaylova, R.S. Bindra, J. Yuan, D. Campisi, L. Narayanan, R. Jensen, F. Giordano, R.S. Johnson, S. Rockwell, P.M. Glazer, Decreased expression of the DNA mismatch repair gene *Mlh1* under hypoxic stress in mammalian cells, Mol. Cell Biol. 23 (2003) 3265–3273.

[12] M. Koshiji, K.K. To, S. Hammer, K. Kumamoto, A.L. Harris, P. Modrich, L.E. Huang, HIF-1α induces genetic instability by transcriptionally downregulating MutSα expression, Mol. Cell 17 (2005) 793–803.

[13] M.F. Goodman, Error-prone repair DNA polymerases in prokaryotes and eukaryotes, Annu. Rev. Biochem. 71 (2002) 17–50.

[14] Y. Zhang, F. Yuan, X. Wu, O. Rechkoblit, J.S. Taylor, N.E. Geacintov, Z. Wang, Error-prone lesion bypass by human DNA polymerase η, Nucleic Acids Res. 28 (2000) 4717–4724.

[15] Y. Zhang, F. Yuan, X. Wu, J.S. Taylor, Z. Wang Z, Response of human DNA polymerase ι to DNA lesions, Nucleic Acids Res. 29 (2001) 928–935.

[16] L. Haracska, L. Prakash, S. Prakash, Role of human DNA polymerase κ as an extender in translesion synthesis, Proc. Natl. Acad. Sci. USA 99 (2002) 16000–16005.

[17] Y. Zhang, X. Wu, D. Guo, O. Rechkoblit, J.S. Taylor, N.E. Geacintov, Z. Wang, Lesion bypass activities of human DNA polymerase μ, J. Biol. Chem. 277 (2002) 44582–44587.

[18] N. Enomoto, N. Koshikawa, M. Gassmann, J. Hayashi, K. Takenaga, Hypoxic induction of hypoxia-inducible factor-1α and oxygen-regulated gene expression in mitochondrial DNA-depleted HeLa cells, Biochem. Biophys. Res. Commun. 297 (2002) 346–352.

[19] J. Chen, S. Zhao, K. Nakada, Y. Kuge, N. Tamaki, F. Okada, J. Wang, M. Shindo, F. Higashino, K. Takeda, M. Asaka, H. Katoh, T. Sugiyama, M. Hosokawa, M. Kobayashi, Dominant-negative hypoxia-inducible factor-1 α reduces tumorigenicity of pancreatic cancer cells through the suppression of glucose metabolism, Am. J. Pathol. 162 (2003) 1283–1291.

[20] T. Fink, A. Kazlauskas, L. Poellinger, P. Ebbesen, V. Zachar, Identification of a tightly regulated hypoxia-response element in the promoter of human plasminogen activator inhibitor-1, Blood 99 (2002) 2077–2083.

[21] Y. Ge, T.L. Jensen, L.H. Matherly, J.W. Taub, Transcriptional regulation of the cystathionine-β-synthase gene in Down syndrome and non-Down syndrome megakaryocytic leukemia cell lines, Blood 101 (2003) 1551–1557.

[22] J.P. McDonald, A. Tissier, E.G. Frank, S. Iwai, F. Hanaoka, R. Woodgate, DNA polymerase ι and related rad30-like enzymes, Philos. Trans R. Soc. Lond. B Biol. Sci. 356 (2001) 53–60.

[23] A. Vaisman, R. Woodgate, Unique misinsertion specificity of polι may decrease the mutagenic potential of deaminated cytosines, EMBO J. 20 (2001) 6520–6529.

[24] T.A. Kunkel, Y.I. Pavlov, K. Bebenek, Functions of human DNA polymerases η, κ and ι suggested by their properties, including fidelity with undamaged DNA templates, DNA Repair (Amst) 2 (2003) 135–149.

[25] A. Tissier, J.P. McDonald, E.G. Frank, R. Woodgate, Polι, a remarkably error-prone human DNA polymerase, Genes Dev. 14 (2000) 1642–1650.

[26] J. Yang, Z. Chen, Y. Liu, R.J. Hickey, L.H. Malkas, Altered DNA polymerase ι expression in breast cancer cells leads to a reduction in DNA replication fidelity and a higher rate of mutagenesis, Cancer Res. 64 (2004) 5597–5607.

[27] X. Lin, K. Ramamurthi, M. Mishima, A. Kondo, S.B. Howell, p53 interacts with the DNA mismatch repair system to modulate the cytotoxicity and mutagenicity of hydrogen peroxide, Mol. Pharmacol. 58 (2000) 1222–1229.

Oncogene (2006) 25, 917–928

www.nature.com/onc

ORIGINAL ARTICLE

Hypoxia selects for high-metastatic Lewis lung carcinoma cells overexpressing Mcl-1 and exhibiting reduced apoptotic potential in solid tumors

N Koshikawa[1,2], C Maejima[1], K Miyazaki[3], A Nakagawara[3] and K Takenaga[1]

[1]Division of Chemotherapy, Chiba Cancer Center Research Institute, Chuoh-ku, Chiba, Japan; [2]Division of Pathology, Chiba Cancer Center Research Institute, Chuoh-ku, Chiba, Japan and [3]Division of Biochemistry, Chiba Cancer Center Research Institute, Chuoh-ku, Chiba, Japan

Low oxygen tension (hypoxia) is a common feature of solid tumors and stimulates the expressions of a variety of genes including those related to angiogenesis, apoptosis and endoplasmic reticulum (ER) stress response. Here we show a close correlation between metastatic potential and the resistance to hypoxia- and ER stress-induced apoptosis among the cell lines with differing metastatic potential derived from Lewis lung carcinoma. An apoptosis-specific expression profiling and immunoblot analyses revealed that the expression of antiapoptotic Mcl-1 increased as the resistance to apoptosis increased. Downregulation of the Mcl-1 expression in the high-metastatic cells by Mcl-1 small interfering RNA increased the sensitivity to hypoxia-induced apoptosis and decreased the metastatic ability. The hypoxia-induced apoptosis was not associated with p53 accumulation, although at present it is not possible to conclude that apoptosis-induced apoptosis is p53-independent. There was no correlation between the expression levels of ER stress-response proteins GADD153, GRP78 and ORP150 and the resistance to hypoxia or ER stresses. *In vitro*, small numbers of the high-metastatic cells overtook the low-metastatic cells after exposure to several rounds of hypoxia and reoxygenation. In solid tumors initially established from equal mixtures, the proportion of the high-metastatic cells to low-metastatic cells was significantly higher in hypoxic areas. Moreover, the high-metastatic cells were overtaking the low-metastatic cells in some of the tumors. Thus, tumor hypoxia and ER stress may provide a physiological selective pressure for the expansion of the high-metastatic cells overexpressing Mcl-1 and exhibiting reduced apoptotic potential in solid tumors.
Oncogene (2006) **25**, 917–928. doi:10.1038/sj.onc.1209128; published online 10 October 2005

Keywords: hypoxia; ER stress; apoptosis; Mcl-1; metastasis

Correspondence: Dr K Takenaga, Division of Chemotherapy, Chiba Cancer Center Research Institute, 666-2 Nitona, Chuoh-ku, Chiba 260-8717, Japan.
E-mail: keizo@chiba-cc.jp
Received 6 January 2005; revised 22 August 2005; accepted 22 August 2005; published online 10 October 2005

Introduction

Response to low oxygen tension (hypoxia) is a fundamental biological phenomenon and therefore hypoxia gives rise to a variety of physiological responses at cellular, local and systemic levels. The cells placed under hypoxic conditions activate many genes including those related to cell survival, glycolysis, angiogenesis, erythrocyte production and iron metabolism to adapt the environment (Semenza, 2000, 2002; Harris, 2002). The oxygen sensing mechanisms have been intensively studied and found to involve hypoxia-inducible factors (HIFs) as key regulatory transcription factors that are composed of HIF-α subunit and HIF-β/aryl hydrocarbon receptor nuclear translocator subunit (Semenza, 2000, 2002; Harris, 2002). HIF binds to the hypoxia-responsive element of hypoxia-responsive genes such as vascular endothelial growth factor (VEGF) and proapoptotic Bnip3, a member of the Bcl-2 family (Semenza, 2000, 2002; Harris, 2002).

Most solid tumors harbor areas of hypoxia, both acute and chronic, due to aberrant vasculature formation and high interstitial pressure (Chaplin and Hill, 1995; Brown and Giaccia, 1998). Although most of the tumor cells die in chronic hypoxia, some of them actually can survive for more than several days in a quiescent or the so-called dormant state (Durand and Sham, 1998) and restart to divide once closed vessels reopen or new vasculatures reach the hypoxic areas. It has been shown that hypoxia induces genetic instability, DNA over-replication and gene amplification in a variety of cultured cells (Rice *et al.*, 1986; Russo *et al.*, 1995; Coquelle *et al.*, 1998). A short-term hypoxia followed by reoxygenation transiently enhances invasive and metastatic potential of some tumor cells (Young and Hill, 1990; Graham *et al.*, 1999; Cairns *et al.*, 2001). Tumor hypoxia selects $p53^{-/-}$ transformed cells and thereby expands cells with diminished apoptotic potential *in vitro* (Graeber *et al.*, 1996). These mechanisms all together are likely to influence the malignant progression of tumor cells (Hill, 1990; Russo *et al.*, 1995; Graeber *et al.*, 1996; Coquelle *et al.*, 1998; Dachs and Chaplin, 1998). Besides, since hypoxic tumor cells cease to divide, they are resistant to conventional radiotherapy and chemotherapy (Rice *et al.*, 1986; Young and Hill, 1990; Teicher, 1994).

Physiological endoplasmic reticulum (ER) stress such as glucose starvation is also present in solid tumors. Hypoxia has been shown to upregulate ER stress-response genes including growth arrest/DNA damage-inducible protein 153 (GADD153/CHOP), which is a proapoptotic transcription factor (Friedman, 1996) and ER chaperones such as glucose-regulated protein (GRP)78/BIP (Munro and Pelham, 1986) and oxygen-regulated protein (ORP)150, which are antiapoptotic proteins (Kuwabara *et al.*, 1996). Upregulation of these ER stress proteins is HIF-independent.

There is accumulating evidence that developing resistance to common apoptotic stimuli is one of the factors that confer high metastatic capability to tumor cells (Glinsky and Glinsky, 1996; McConkey *et al.*, 1996; Bufalo *et al.*, 1997; Glinsky, 1997; Inbal *et al.*, 1997; Shtivelman, 1997; Takaoka *et al.*, 1997; Fernandez *et al.*, 2000; Lowe and Lin, 2000; Wong *et al.*, 2001). The apoptosis-resistant phenotype may be advantageous for tumor cells to survive in the metastatic process. We reported that the high-metastatic clone (A11 cells) established from Lewis lung carcinoma is more resistant to apoptosis induced by serum starvation, hypoxia and glucose deprivation than the low-metastatic clone (P29 cells) (Takasu *et al.*, 1999). However, it remained to be examined whether there is a correlation between metastatic ability and resistance to apoptosis induced by various stresses among various clones with differing metastatic potential. In addition, molecular mechanisms of the apoptosis resistance of the high-metastatic cells remained obscure. We addressed here these points and, furthermore, if hypoxia could act as a physiological selective pressure in solid tumors for the expansion of high-metastatic tumor cells that possess diminished apoptotic potential. The results showed that the high-metastatic Lewis lung carcinoma cell lines are more resistant to hypoxia- and ER stress-induced apoptosis than the low-metastatic cell lines, that the high-metastatic cells overexpress antiapoptotic Mcl-1, and that hypoxia selects for the high-metastatic cells in solid tumors.

Results

Correlation between metastatic potential and resistance to hypoxia- and ER stress-induced apoptosis in the low- and high-metastatic cell lines

To investigate the correlation between susceptibility to hypoxia-induced cell death and metastatic potential, we exposed the five cell lines with differing metastatic potential derived from a mouse Lewis lung carcinoma (metastatic capability; P29 = P34 < C2 < D6 < A11) to hypoxia (~0.1% O_2), corresponding to oxygen concentrations commonly found in solid tumors. Cell death was monitored after culturing the cell lines for 72 h under hypoxia. The results showed that only less than 8% of P29 and P34 cells were viable while about 20% of C2 cells and over 45% of D6 and A11 cells remained viable (Figure 1a). Thus, we observed a tendency where the resistance to hypoxia-induced cell death is correlated with the metastatic ability. The time course showed that hypoxia induced cell death more rapidly in P29 cells than in A11 cells (Figure 1b). Clonogenic assays in which the cells were exposed to hypoxia for 3 or 4 days and then reoxygenated to form colonies also demonstrated that A11 cells survived longer than P29 cells under hypoxic conditions (Figure 1c). The cells positive for annexin V and TUNEL staining increased in hypoxic P29 cells (Figure 1d). An increase in the number of cells exhibiting chromatin condensation and fragmentation as assessed by DAPI staining was also observed in hypoxic P29 cells (0.1 and 26.1% for normoxic and hypoxic P29 cells, respectively) (Figure 1d). In addition, flow cytometric analysis revealed an increase in the percentage of sub-G1 population in these cells (0.7 and 20.6% for normoxic and hypoxic cells, respectively) (Figure 1e). Thus, these data indicate that hypoxic P29 cells were dying through apoptosis. We confirmed that hypoxic A11 cells died of apoptosis based on the same criteria.

To test whether the high-metastatic cell lines are also resistant to ER stresses compared with the low-metastatic cell lines, we treated P29, P34, D6 and A11 cells with chemical ER stress inducers for 2 days and examined their viability. As shown in Figure 2, compared to P29 and P34 cells, D6 and A11 cells were much more resistant to apoptosis induced by tunicamycin (5 μg/ml), brefeldin A (5 μg/ml), thapsigargin (250 nM) and A23187 (1 μM).

Mcl-1 is overexpressed in the high-metastatic cell lines

To find out the genes responsible for the susceptibility to hypoxia-induced apoptosis, we compared the expression profile of apoptosis-related genes among normoxic and hypoxic P29 and A11 cells using a cDNA expression microarray cumulated apoptosis-related genes. The data showed that A11 cells expressed antiapoptotic *Mcl-1* gene at higher levels than P29 cells (not shown). Immunoblot analysis confirmed a higher expression of Mcl-1 in A11 cells than in P29 cells under both normoxic and hypoxic conditions (Figure 3A). We detected two close bands (40 and 37 kDa) on the blots. Since the expressions of the bands were decreased by treatment with Mcl-1 siRNA (see below), the 37 kDa band may be a degradation product of Mcl-1 or, though less likely, a splicing variant of *Mcl-1* gene. It is of note that the cell lines expressed Mcl-1 (40 kDa) at the levels according to the resistance to hypoxia- and other stress-induced apoptosis (Figure 3A and B). Consistent with the recent report that hypoxia enhances Mcl-1 expression in hepatoma HepG2 cells through HIF-1 (Piret *et al.*, 2005), the amount of Mcl-1 was increased by hypoxia in C2, D6 and A11 cells (Figure 3B). Immunohistochemistry for Mcl-1 on the sections prepared from paraffin-embedded P29 and A11 tumors showed a higher expression of Mcl-1 in A11 cells than in P29 cells, indicating that Mcl-1 overexpression is persistent even *in vivo* (Figure 3C).

The expression profiling also showed that hypoxia induced proapoptotic *Bnip3* gene expression in both P29

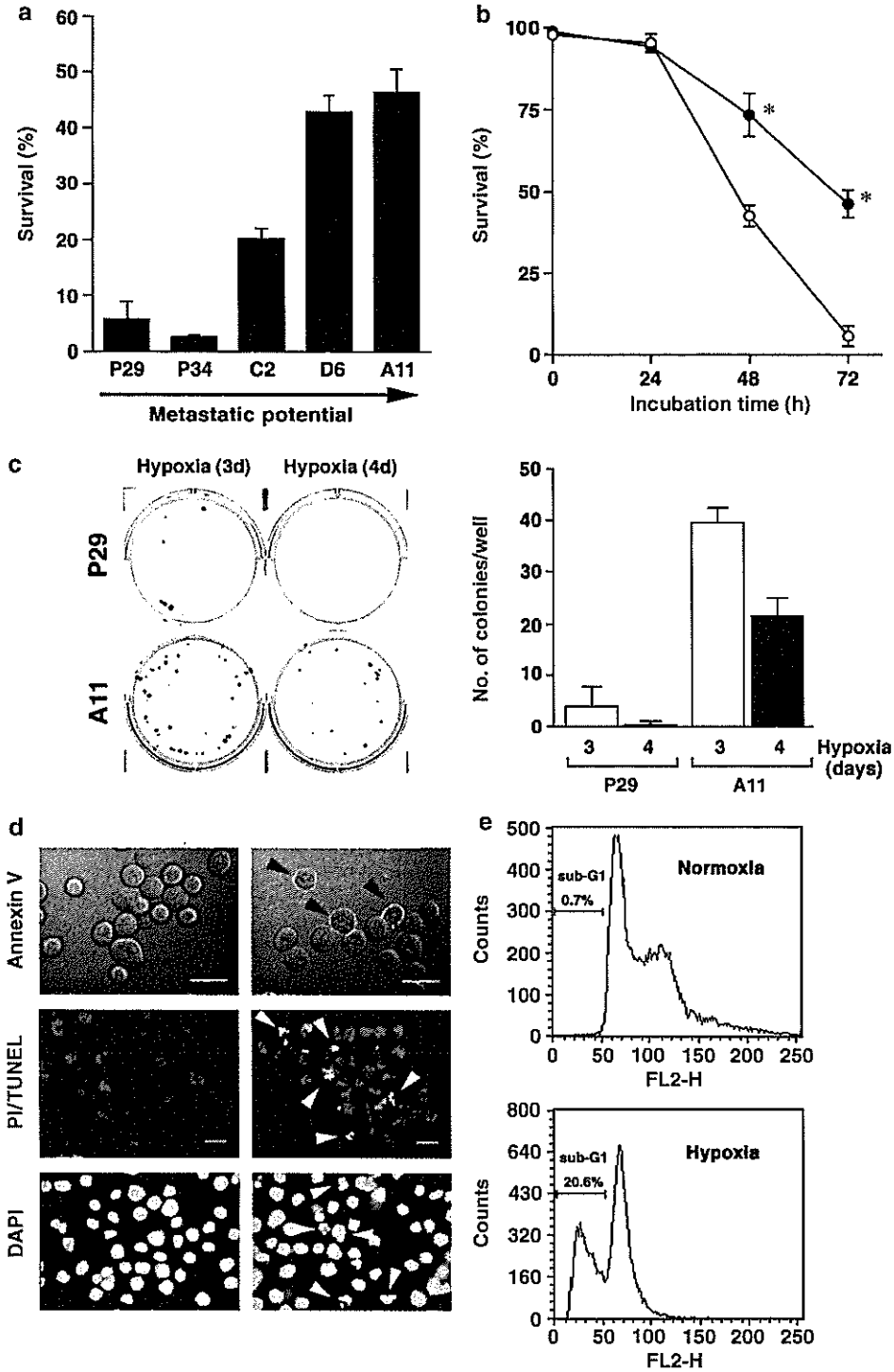

Figure 1 Sensitivity to hypoxia-induced apoptosis of the Lewis lung carcinoma cell lines. (a) Hypoxia-induced cell death of the cell lines with differing metastatic potential. The cell lines were exposed to hypoxia for 72 h. Percentage of living cells was determined on the basis of trypan blue exclusion. Bars; s.d. of triplicate determinations. (b) Time course of cell death induced by hypoxia. P29 (○) and A11 cells (•) were exposed to hypoxia for the indicated time period. Percentage of living cells was determined on the basis of trypan blue exclusion Bars; s.d. of triplicate determinations. *Significant at $P<0.002$. (c) Clonogenic assay of cell survival. P29 and A11 cells (100 cells/well) were cultured under hypoxic conditions for 3 or 4 days followed by culturing under normoxic conditions. Colonies were stained with crystal violet (left panel) and then counted (right panel). Bars; s.d. of triplicate determinations. (d) Annexin V, TUNEL and DAPI stainings of normoxic (left panels) and hypoxic P29 cells (right panels). P29 cells were cultured under hypoxic conditions for 18, 27 or 28 h, and then stained for annexin V-EGFP, TUNEL (green) and PI (red), or DAPI, respectively. Arrowheads show apoptotic cells. (e) Flow cytometric analysis of DNA fragmentation. P29 cells cultured under hypoxic conditions for 27 h were subjected to FACscan analysis. The percentage of sub-G1 fraction is also shown.

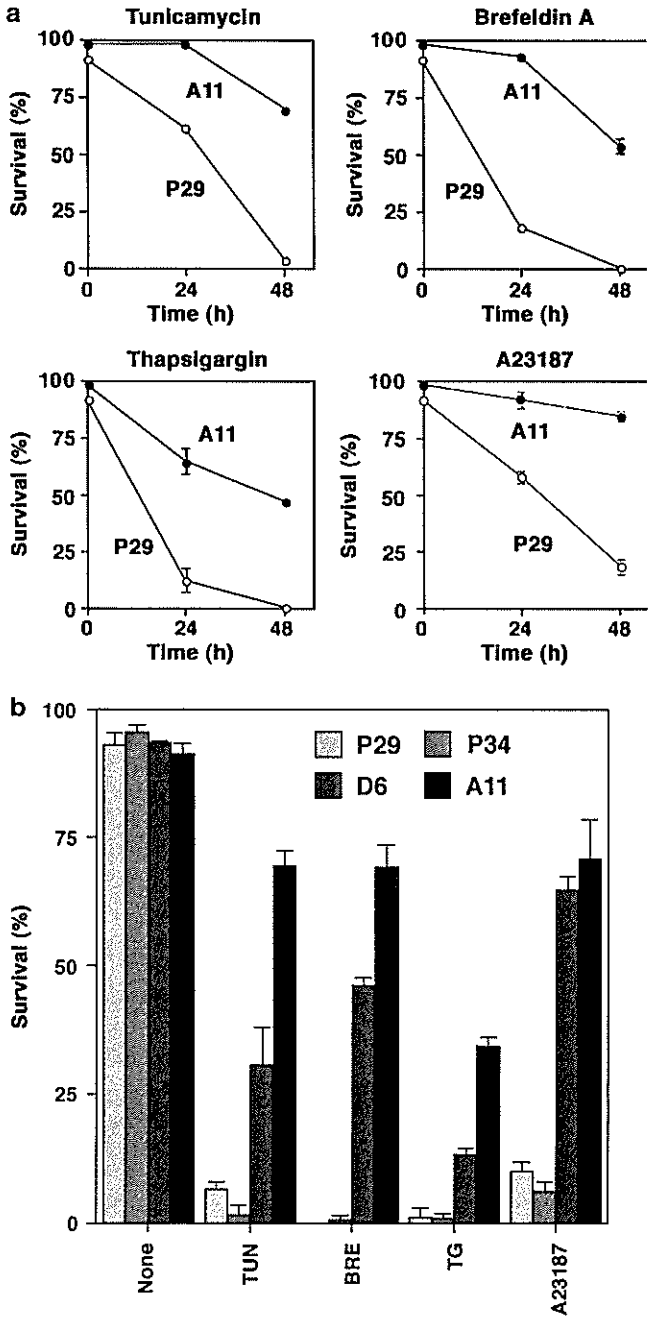

Figure 2 Sensitivity to ER stress-induced apoptosis of the Lewis lung carcinoma cell lines. (a) Time course of cell death of P29 (○) and A11 cells (•) exposed to ER stress-inducing agents. The cells were exposed to tunicamycin (5 μg/ml), brefeldin A (5 μg/ml), thaspigargin (250 nM), A23187 (1 μM)). (b) Sensitivity of the cell lines with differing metastatic potential to ER stress-inducing agents. P29, P34, D6 and A11 cells were exposed to tunicamycin (5 μg/ml), brefeldin A (5 μg/ml), thaspigargin (250 nM), A23187 (1 μM)) for 2 days. Percentage of living cells was determined on the basis of trypan blue exclusion. Bars; s.d. of triplicate determinations.

and A11 cells (data not shown). Actually, *Bnip3* mRNA expression was induced in all of the cell lines, but the expression level was not correlated with the susceptibility to hypoxia- and other stress-induced apoptosis (Figure 3D).

To investigate whether the hypoxia-induced apoptosis is associated with p53 accumulation, we examined the expression of p53 in hypoxia- and doxorubicin-treated P29, P34, D6 and A11 cells. Immunoblot analysis revealed that hypoxia reduced p53 expression (Figure 3E) and failed to induce endogenous downstream p53 effector proteins, Bax and $p21^{WAF1/CIP1}$, in these cell lines (not shown). By contrast, doxorubicin caused the accumulation of p53 (Figure 3E).

We next compared the expression levels of ER stress-response proteins, GADD153, GRP78 and ORP150, which are known to be induced by hypoxia, between P29 and A11 cells. As shown in Figure 3F and G, the expressions of these proteins were induced by tunicamycin and hypoxia, but there was no difference between 29 and A11 cells.

Effects of Mcl-1 siRNA on hypoxia-induced apoptosis and metastatic potential

To examine if the expression of Mcl-1 is responsible for the resistance to hypoxia-induced apoptosis, we transfected A11 cells with either Mcl-1 siRNA or control siRNA. As shown in Figure 4a and b, the expression of Mcl-1 was suppressed by Mcl-1 siRNA, but not by control siRNA. We then cultured these cells under hypoxic conditions for 60 h and monitored cell death. The results showed that Mcl-1 siRNA-treated A11 cells were more sensitive to hypoxia-induced apoptosis than mock and control siRNA-treated cells in both normal growth medium and serum-starved medium (Figure 4c). Importantly, Mcl-1 siRNA-treated A11 cells were less metastatic than control siRNA-treated cells, as assessed by lung weight and the number of metastatic nodules in the lung (Figure 4d). Thus, it appeared that Mcl-1 is at least in part involved in resistance to hypoxia-induced apoptosis and metastatic potential of A11 cells.

Apoptosis of the low- and high-metastatic cells in hypoxic areas of solid tumors

To examine whether the difference in the susceptibility to hypoxia-induced apoptosis can also be observed *in vivo*, we injected EF5, a nitroimidazole compound, into mice bearing subcutaneous P29 or A11 tumors of nearly equal size for detecting hypoxic areas and stained cryosections of the tumors first with TUNEL assay using fluorescein-labeled nucleotides, and then with Cy3-labeled antibodies against EF5-cellular macromolecule adducts (Figure 5a). EF5 binding occurs under low-oxygen conditions and only in viable cells (Lord *et al.*, 1993). The number of TUNEL-positive cells per 100 μm^2 in EF5-positive (hypoxic) and -negative (normoxic) areas was counted (Figure 5b). We omitted necrotic areas from the investigation. The results showed that the number of apoptotic cells in hypoxic areas of P29 tumors was fourfold larger than that in hypoxic areas of A11 tumors. In normoxic areas, the number of apoptotic cells was small but statistically larger in P29 tumors than in A11 tumors.

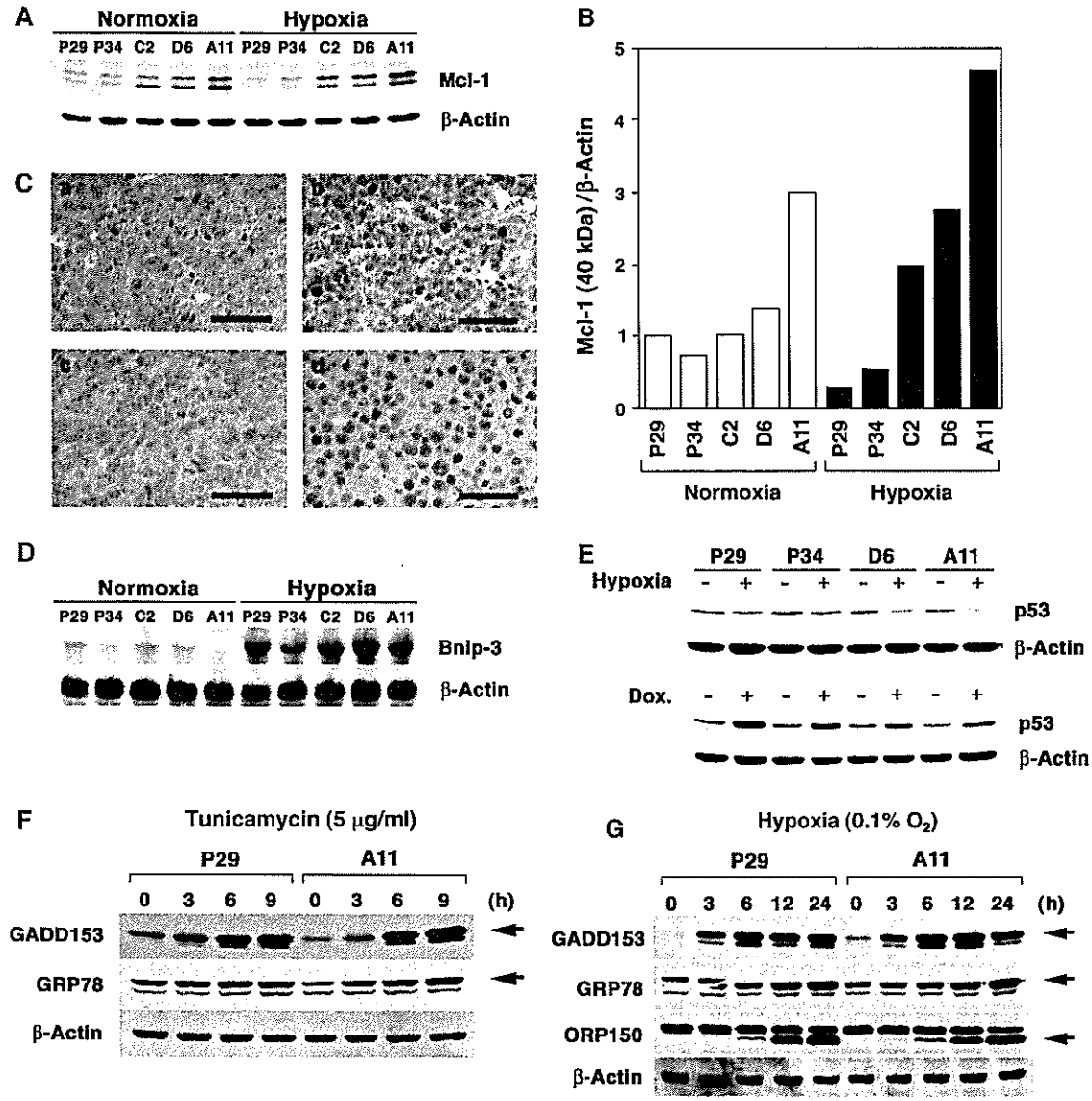

Figure 3 Expressions of apoptosis-related genes in Lewis lung carcinoma cell lines. (**A**) Western blot analysis of the effect of hypoxia on Mcl-1 expression. The cells exposed to hypoxia (~0.1% O_2) for 8 h were subjected to immunoblot analysis for Mcl-1 expression. β-actin served as loading controls. (**B**) Relative values for signal intensity of Mcl-1 (40 kDa) after normalization to the level of β-actin. Scanning densitometry of the gel was performed and the normalized values were represented by the white (under normoxia) and black (under hypoxia) bars. All values are shown as a percentage of the value for normoxic P29 cells. The results are representative of two separate experiments in which similar results were obtained. (**C**) Immunohistochemical analysis of Mcl-1 expression in P29 and A11 tumors. Sections from P29 tumors (a and c) and A11 tumors (b and d) were immunostained with anti-Mcl-1 antibody (a and b) and control IgG (c and d). Bars; 50 μm. (**D**) Effects of hypoxia on *Bnip3* mRNA expression. The cells exposed to hypoxia (0.1% O_2) for 8 h were subjected to Northern analysis for Bnip3 mRNA expression. β-Actin mRNA served as loading controls. (**E**) Western blot analysis of the effects of hypoxia and doxorubicin on the accumulation of p53 protein. The cells exposed to hypoxia (0.1% O_2) for 24 h or 5 μg/ml doxorubicin (Dox) for 20 h were subjected to immunoblot analysis for p53 expression. β-Actin served as loading controls. (**F**) Western blot analysis of the effects of tunicamycin on the expressions of GADD153 and GRP78. P29 and A11 cells were exposed to 5 μg/ml tunicamycin for the indicated periods of time. βActin served as loading controls. (**G**) Western blot analysis of the effects of hypoxia on the expressions of GADD153, GRP78 and ORP150. P29 and A11 cells were exposed to hypoxia (0.1% O_2) for the indicated periods of time. β-actin served as loading controls.

Survival advantage of the high-metastatic cells under hypoxic conditions

The above results prompted us to examine whether A11 cells have a survival advantage over P29 cells under hypoxic conditions. To this end, we established genetically labeled P29 ($P29^{EGFP}$ cells) and A11 cells ($A11^{IRES\text{-}EGFP}$ cells) after selecting P29 and A11 cells stably transfected with pEGFP-N1 and pIRES2-EGFP, respectively (Figure 6a), and characterized their properties. $P29^{EGFP}$ cells grew faster than $A11^{IRES\text{-}EGFP}$ cells *in vivo*, and at 17 days after tumor cell inoculation $P29^{EGFP}$ tumors were twice larger than $A11^{IRES\text{-}EGFP}$ tumors (Figure 6b). $P29^{EGFP}$ tumors contained large necrotic regions. $P29^{EGFP}$ and $A11^{IRES\text{-}EGFP}$ cells were low- and

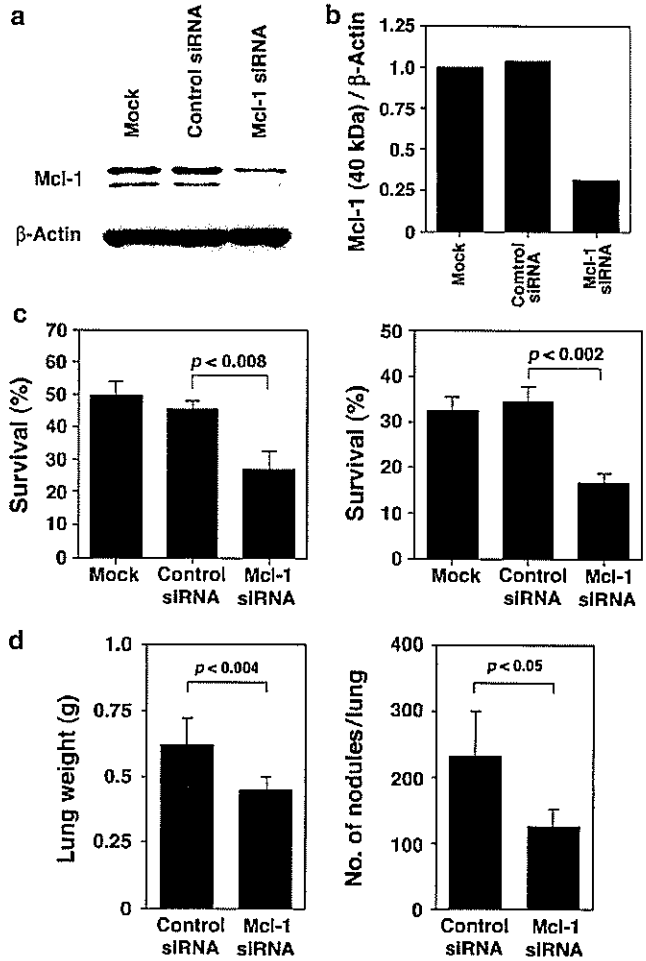

Figure 4 Effects of Mcl-1 siRNA on hypoxia-induced apoptosis and metastatic potential of A11 cells. (a) Expression of Mcl-1 in A11 cells treated with Mcl-1 siRNA. A11 cells pretreated with Lipofectamine 2000 alone (mock), 25 nM control siRNA or 25 nM Mcl-1 siRNA for 2 days were subjected to immunoblot analysis for Mcl-1 expression. β-Actin served as loading controls. (b) Relative values for signal intensity of Mcl-1 (40 kDa) after normalization to the level of β-actin. Scanning densitometry of the gel was performed and the relative values were represented. All values are shown as a percentage of the value for mock-transfected A11 cells. The results are representative of three separate experiments in which similar results were obtained. (c) Sensitivity of Mcl-1 siRNA-treated A11 cells to hypoxia-induced apoptosis. A11 cells pretreated with Lipofectamine 2000 alone (mock), 25 nM control siRNA or 25 nM Mcl-1 siRNA for 2 days were cultured under hypoxic conditions (~0.1% O_2) for 60 h in normal growth medium (left panel) or serum-starved (1% serum) medium (right panel). Cell death was examined by trypan blue staining. Bars; s.d. of triplicate determinations. (d) Metastatic potential of Mcl-1 siRNA-treated A11 cells. A11 cells pretreated with 25 nM control siRNA or 25 nM Mcl-1 siRNA for 2 days were injected intravenously into C57BL/6 mice (6 mice/group). At 17 days after the injection, the weight of the lungs (left panel) and the number of metastatic nodules (right panel) were measured. Bars; s.d.

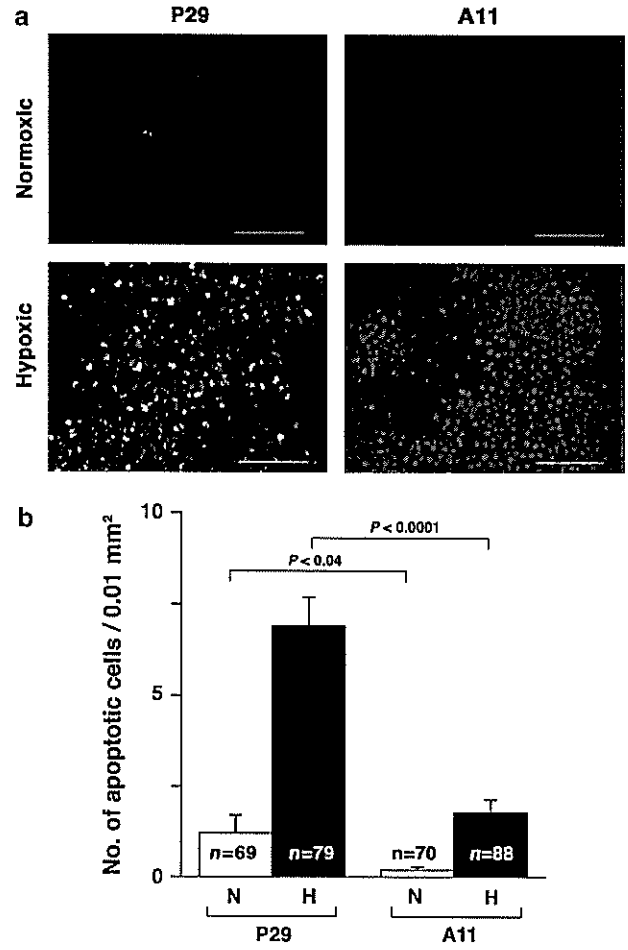

Figure 5 Apoptosis of P29 and A11 cells in tumor hypoxic areas. (a) TUNEL staining (green) and EF5 staining (red) of frozen sections of subcutaneous tumors established from P29 and A11 cells. (b) Frequency of apoptotic (TUNEL-positive) cells in normoxic (N) and hypoxic (H) areas. Bars; s.e.m.

high-metastatic, respectively, in both experimental and spontaneous metastasis assays (Figure 6c) and showed a similar apoptosis resistance to their parental cells (Figure 6d).

To obtain a standard curve by which the percentage of $A11^{IRES\text{-}EGFP}$ cells in mixtures of unknown proportions of $P29^{EGFP}$ and $A11^{IRES\text{-}EGFP}$ cells could be calculated, we extracted genomic DNA from mixtures of known proportions of the cells and performed PCR followed by Southern blot with an EGFP probe (Figure 6e). By plotting the relative intensities of the bands corresponding to EGFP and IRES-EGFP against the known proportion of $A11^{IRES\text{-}EGFP}$ cells, a standard curve, although slightly sigmoid, was obtained (Figure 6f). The value at each point did not significantly fluctuate even when we carried out PCR under various conditions (1–100 ng DNA, 20–35 PCR cycles) (not shown).

We then mixed $A11^{IRES\text{-}EGFP}$ and $P29^{EGFP}$ cells at a 1:1, 1:10 or 1:100 ratio and treated them with multiple rounds of hypoxia and reoxygenation (recovery in normoxia). The percentage of $A11^{IRES\text{-}EGFP}$ cells at the time of cell harvesting was determined from the standard curve after quantitation of radioactive intensity of the PCR bands. We found that the percentage of $A11^{IRES\text{-}EGFP}$ cells increased dramatically after several rounds of hypoxia-reoxygenation in every case (Figure 7a and b). The intensity of the band corresponding to EGFP and IRES-EGFP in $P29^{EGFP}$ and $A11^{IRES\text{-}EGFP}$

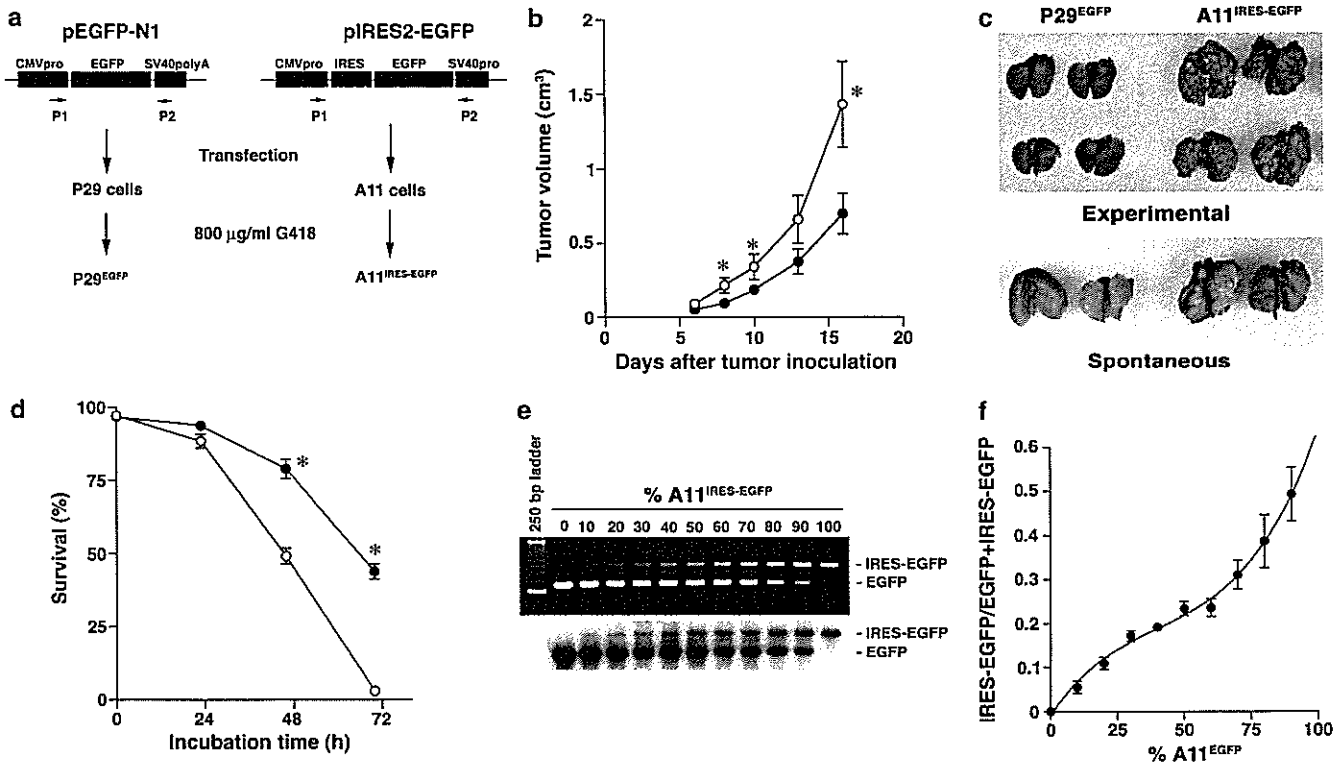

Figure 6 Establishment and properties of $P29^{EGFP}$ and $A11^{IRES\text{-}EGFP}$ cells. (a) Schematic drawings of the establishment of $P29^{EGFP}$ and $A11^{IRES\text{-}EGFP}$ cells and the primers, P1 and P2, used for PCR. (b) *In vivo* growth of $P29^{EGFP}$ and $A11^{IRES\text{-}EGFP}$ cells. $P29^{EGFP}$ (○) and $A11^{IRES\text{-}EGFP}$ cells (•) (2.5×10^5) were injected subcutaneously into C57BL/6 mice (7 mice/group). Bars; s.e.m. *Significant at $P<0.04$. (c) Metastatic potential of $P29^{EGFP}$ and $A11^{IRES\text{-}EGFP}$ cells. For experimental metastasis, the cells (2×10^5 cells/mouse) were injected intravenously, and the lungs were excised 17 days after the injection. For spontaneous metastasis, the cells (2×10^5 cells/mouse) were inoculated subcutaneously, and the lungs were excised 30 days after the inoculation. (d) Hypoxia-induced apoptosis of $P29^{EGFP}$ (○) and $A11^{IRES\text{-}EGFP}$ cells (•). Percentage of living cells was determined on the basis of trypan blue exclusion. Bars; s.d. of triplicate determinations. *Significant at $P<0.003$. (e) Ethidium bromide staining and Southern blot of PCR fragments amplified using genomic DNA extracted from mixtures of known proportions of $P29^{EGFP}$ and $A11^{IRES\text{-}EGFP}$ cells. (f) A standard curve by which the percentage of $A11^{IRES\text{-}EGFP}$ cells in a mixed culture or a tumor could be calculated. The relative intensities of the bands shown in (e) were plotted against the known proportion of $A11^{IRES\text{-}EGFP}$ cells. Bars; s.d. of three independent experiments.

cells, respectively, treated with the same protocol was constant (Figure 7c), indicating that the integrated marker genes was stable.

Survival advantage of the high-metastatic cells in solid tumors

We next examined the proportion of $A11^{IRES\text{-}EGFP}$ cells in normoxic and hypoxic areas of solid tumors established from a 1:1 mixture of $P29^{EGFP}$ and $A11^{IRES\text{-}EGFP}$ cells. Since $P29^{EGFP}$ cells grew faster than $A11^{IRES\text{-}EGFP}$ cells *in vivo* (Figure 6b), the percentage of $A11^{IRES\text{-}EGFP}$ cells in both normoxic and hypoxic areas of the heterogeneous tumors should be lower than 50% if no selection of cells occurs in the tumors. We cut out EF5-negative and -positive areas (approximately total 1 mm^2) from cryosections of the tumors excised at 17 days after tumor inoculation by using laser-assisted microdissection, extracted genomic DNA, and then examined the percentage of $A11^{IRES\text{-}EGFP}$ cells in these areas as described above (Figure 8a and b). The data showed that the proportion of $A11^{IRES\text{-}EGFP}$ cells in normoxic areas decreased from the initial 50% in five out of the seven mixed tumors. However, the proportion was over 70% in #2 and #5 tumors (Figure 8b). Intriguingly, the percentage of $A11^{IRES\text{-}EGFP}$ cells in hypoxic areas was quite high in five out of the seven tumors. Overall, the proportion of $A11^{IRES\text{-}EGFP}$ cells in normoxic and hypoxic areas was 36.4 ± 26.0 and $69.0 \pm 21.0\%$, respectively ($P<0.011$). The intensity of bands corresponding to EGFP and IRES-EGFP of the cells collected from normoxic and hypoxic areas of $P29^{EGFP}$ and $A11^{IRES\text{-}EGFP}$ tumors was constant (Figure 8c), indicating that the integrated marker genes was also stable *in vivo*. Thus, $A11^{IRES\text{-}EGFP}$ cells showed a clear survival advantage over $P29^{EGFP}$ cells in hypoxic areas.

The loss of $P29^{EGFP}$ cells in normoxic areas of some heterogeneous tumors (#2 and #5 tumors) suggests a possibility that a greater portion of $P29^{EGFP}$ cells was lost in the tumors. To test this possibility, we extracted genomic DNA from the whole tumors and examined the proportion of $A11^{IRES\text{-}EGFP}$ cells. The results showed that the proportion was over 90% in #2 tumor, indicating that $A11^{IRES\text{-}EGFP}$ cells nearly overtook $P29^{EGFP}$ cells in this tumor (Figure 8d and e). In #5 tumor, it was below 50%. This and the above results suggest that $A11^{IRES\text{-}EGFP}$

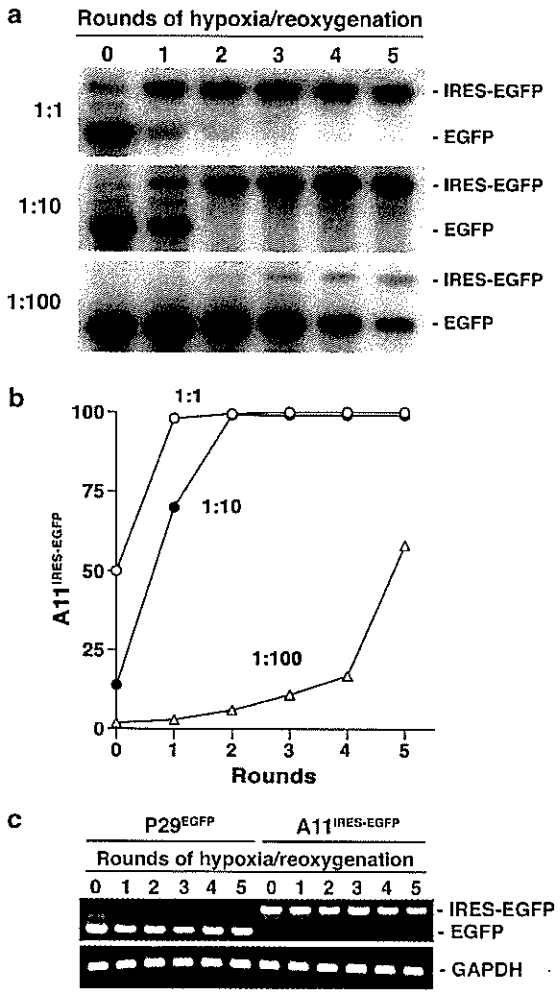

Figure 7 Hypoxia-reoxygenation selects $A11^{IRES\text{-}EGFP}$ cells in a mixed culture. (a) Southern blot of PCR fragments amplified using genomic DNA extracted from mixtures of $P29^{EGFP}$ and $A11^{IRES\text{-}EGFP}$ cells. $A11^{IRES\text{-}EGFP}$ were mixed with $P29^{EGFP}$ cells at a 1:1, 1:10 or 1:100 ratio and treated with multiple rounds of hypoxia-reoxygenation. (b) Selection of $A11^{IRES\text{-}EGFP}$ cells following hypoxia-reoxygenation treatment. The percentage of $A11^{IRES\text{-}EGFP}$ cells was calculated by the standard curve shown in Figure 6f after measuring the relative intensities of the PCR bands shown in (a). The data are representative of two separate experiments in which similar results were obtained. (c) Stability of the integrated marker genes in $P29^{EGFP}$ and $A11^{IRES\text{-}EGFP}$ cells. Ethidium bromide staining of the PCR bands is shown.

cells nearly overtook $P29^{EGFP}$ cells only in the local normoxic areas that were dissected by microdissection. The percentage of $A1^{IRES\text{-}EGFP}$ cells was over 50% in #1 and #6 tumors, suggesting that the cells were overtaking $P29^{EGFP}$ cells in these tumors. In other 3 tumors, the percentage was below 50%, indicating that selection of $A11^{IRES\text{-}EGFP}$ cells was occurring in local hypoxic areas of these tumors but was not apparent in whole tumor mass.

Discussion

The data presented here showed a close correlation between metastatic potential and the resistance to hypoxia-induced apoptosis among the cell lines with differing metastatic potential. They also showed that the high-metastatic cells are more resistant to ER stress-induced apoptosis. The hypoxia-induced apoptosis may be p53-independent, because hypoxia neither caused p53 accumulation nor induced the expressions of endogenous downstream p53 effector proteins. An apoptosis-specific expression profiling and immunoblot analyses demonstrated a correlation between the resistance to hypoxia-induced apoptosis and the expression level of Mcl-1. Downregulation of the Mcl-1 expression in A11 cells by Mcl-1 siRNA increased the sensitivity to hypoxia-induced cell death and, importantly, decreased the metastatic ability. Although there are so far few reports directly indicating the involvement of Mcl-1 in metastatic potential of tumor cells, a clinicopathological study suggested Mcl-1 as an indicator of tumor progression and prognosis in patients with gastric carcinoma (Maeta *et al*., 2004). Therefore, Mcl-1 may be one of the factors that confer metastatic potential on at least some tumor cells.

In agreement with the previous reports (Bruick, 2000; Guo *et al*, 2001), hypoxia induced the expression of Bnip3 in all of the cell lines used in this study. Bnip3 is a mitochondrial protein and induces apoptosis independently of Apaf-1, cytochrome *c* release and caspase activation (Vande Velde *et al*., 2000). Bcl-2 and Bcl-X_L bind to Bnip3 and inhibit apoptosis caused by the overexpression of Bnip3 (Ray *et al*., 2000). Therefore, it is possible that Mcl-1 binds to Bnip3 and inhibits Bnip3-induced apoptosis. We preliminarily examined this possibility, and the data showed that Mcl-1 physically interacts with Bnip3 (data not shown).

There was no difference in the inducibility of ER stress- and hypoxia-inducible genes such as GADD153, GRP78 and ORP150 genes between the low- and the high-metastatic cell lines, eliminating the involvement of these genes in the difference of the sensitivity to hypoxia- and ER-stress-induced apoptosis.

The present results clearly demonstrated the survival advantage of A11 cells over P29 cells. In the mixed culture, A11 cells overtook P29 cells during several rounds of hypoxia-reoxygenation. It would be of interest to note that as the rounds of selection proceeded A11 cells progressively became more resistant to apoptosis induced by not only hypoxia but also serum starvation, glucose deprivation and anticancer drugs such as cisplatin and etoposide (not shown). Therefore, it is likely that repeated exposure to hypoxia-reoxygenation results in the selection of not merely A11 cells with original phenotype but of A11 cells with more malignant phenotype, consistent with previous reports (Kim *et al*., 1997; Kinoshita *et al*., 2001).

Coinciding with the *in vitro* experiments, the frequency of apoptosis was greater in the hypoxic areas of A11 tumors than in those of P29 tumors. Intriguingly, it appeared that A11 cells became a majority in the hypoxic areas of many tumor masses established from equal mixtures of P29 and A11 cells. It is of note that although we randomly excised the hypoxic areas the proportion of A11 cells in these areas was over 90% in

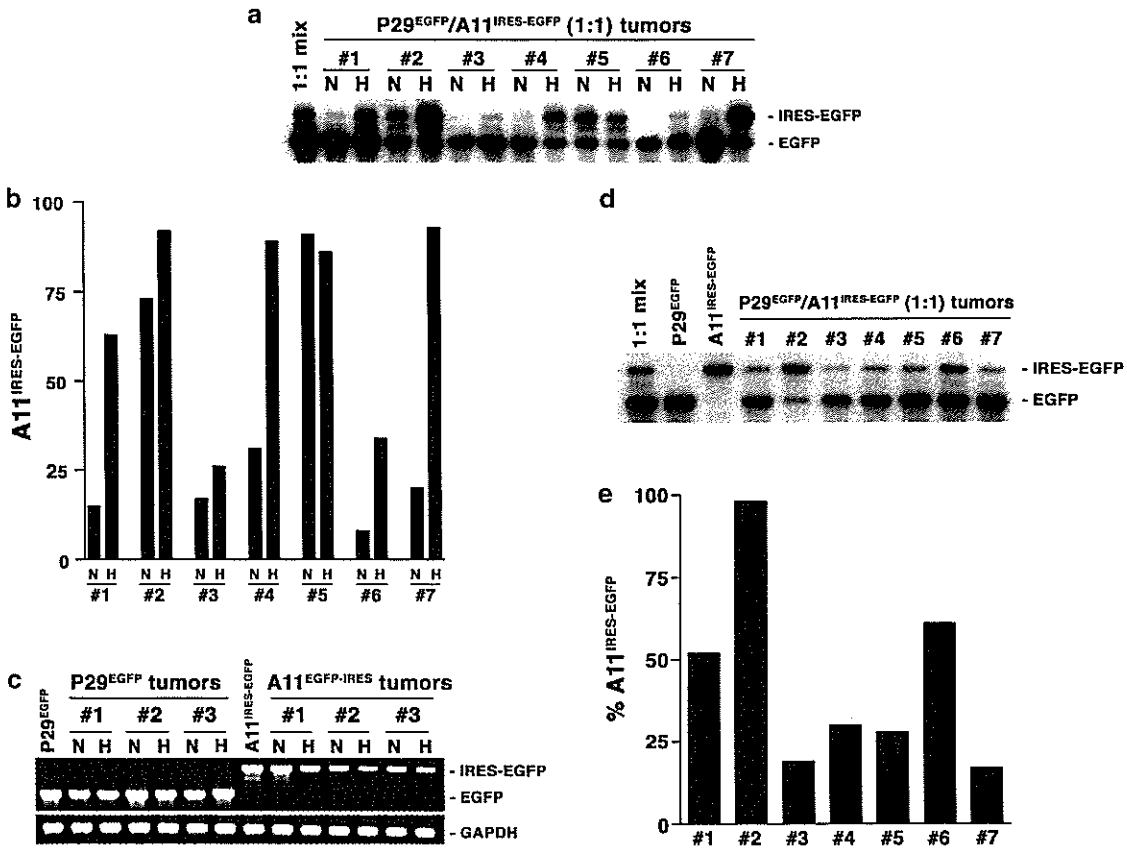

Figure 8 Proportion of A11$^{IRES\text{-}EGFP}$ cells in tumors. (a) Southern blot of PCR fragments amplified using genomic DNA extracted from normoxic (N) and hypoxic (H) areas in subcutaneous tumors established from equal mixtures of P29^{EGFP} and A11$^{IRES\text{-}EGFP}$ cells. (b) The percentage of A11$^{IRES\text{-}EGFP}$ cells in normoxic (N) and hypoxic (H) areas in subcutaneous tumors. The percentage of A11$^{IRES\text{-}EGFP}$ cells was calculated by the standard curve shown in Figure 5f after measuring the relative intensities of the PCR bands shown in (a). (c) Stability of the integrated marker genes in normoxic (N) and hypoxic (H) areas of P29^{EGFP} and A11$^{IRES\text{-}EGFP}$ tumors. Ethidium bromide staining of the PCR bands is shown. (d) Southern blot of PCR fragments amplified using genomic DNA extracted from subcutaneous tumors established from equal mixtures of P29^{EGFP} and A11$^{IRES\text{-}EGFP}$ cells. (e) The percentage of A11$^{IRES\text{-}EGFP}$ cells in subcutaneous tumors. The percentage of A11$^{IRES\text{-}EGFP}$ cells was calculated by the standard curve shown in Figure 6f after measuring the relative intensities of the PCR bands shown in (d). Tumor numbers (#) correspond to those in (a).

several samples. This was somewhat surprising. We had expected that the proportion would vary widely from one sample to another, because the time of hypoxia influences the degree of apoptosis and EF5-binding does not tell us how long hypoxia had lasted in EF5-positive areas before excision. Nevertheless, a majority of P29 cells was commonly lost in the randomly selected hypoxic areas. One possible explanation for this is that P29 cells die more rapidly in *in vivo* hypoxic areas in which starvation of growth factors and nutrients that could act synergistically with hypoxia to induce apoptosis also occurs. We then exposed P29 and A11 cells to serum starvation (0.5% FBS) and hypoxia (0.1% O_2) simultaneously. The data showed that more than 75% of P29 cells died within 24 h while more than 70% of A11 cells survived. Thus, P29 cells are less tolerant towards severer conditions in *in vivo* hypoxic areas than A11 cells, and this might explain the rapid loss of P29 cells in hypoxic areas. Interestingly, we observed two cases out of the seven tumors in which A11 cells dominated in not only hypoxic areas but also normoxic areas. It is possible that the normoxic areas represent the ones that are reoxygenated after hypoxia. Intriguingly, in one case (#2 tumor), the proportion of A11 cells in the tumor mass was over 90%. This suggests that a majority of P29 cells died of apoptosis induced by severe hypoxia and other microenvironmental factors in the early phase of growth of this tumor, resulting in the selection of A11 cells. The degree of tumor vascularization and angiogenesis may vary from one tumor to another even if they are established from the same tumor cells, and accordingly the extent of hypoxia may differ in individual tumor. This may explain the difference in the proportion of A11 cells in each tumor.

It has been reported that hypoxia induces p53-dependent apoptosis and thus selects *p53*$^{-/-}$ cells (Graeber *et al.*, 1996). Our study showed that hypoxia selects for cells with reduced apoptotic potential and high-metastatic ability. This phenomenon could occur in human tumors such as cervical cancer, head and neck cancer and soft tissue sarcoma in which a correlation between hypoxia and aggressiveness or poor prognosis has been reported (Brizel *et al.*, 1996, 1997; Höckel

et al., 1996, 1999). Therefore, the data presented here may have important implications for malignant progression of tumors.

Materials and methods

Cell culture
The cell lines, P29, P34, C2, D6 and A11, established from Lewis lung carcinoma, have been characterized elsewhere (Takasu *et al.*, 1999; Koshikawa *et al.*, 2003). They were grown in Dulbecco's modified Eagle's medium (DMEM) containing 10% fetal bovine serum supplemented with 100 units/ml penicillin and 100 μg/ml streptomycin. Cells were cultured at 37°C in a humidified atmosphere with 5% CO_2 or under hypoxic conditions (ca. 0.1% O_2) generated in BBL GasPak Pouch (Becton Dickinson Microbiology Systems, Cockeysville, MA, USA). In some experiments, they were treated with tunicamycin (Sigma-Aldrich, St Louis, MO, USA), brefeldin A (WAKO Pure Chemical Industries, Ltd., Osaka, Japan), thapsigargin (Sigma-Aldrich), A23187 (Sigma-Aldrich) or vehicle alone.

Assessment of cell viability and apoptosis
Cells were seeded at a concentration of 3×10^5 cells/dish (Falcon 3002), and cell death was induced by culturing them under hypoxic conditions or in the presence of various drugs. For aerobic recovery, the cells were cultured in normoxia until they become subconfluent, thus the recovery time was different for each cell line. Cell viability was assessed by trypan blue dye exclusion. Flow cytometric analysis was performed as described previously (Takasu *et al.*, 1999) to detect cellular DNA fragmentation with a FACScan flow cytometer (Becton Dickinson, Mountain View, CA, USA). Chromatin condensation and fragmentation were visualized by staining the cells with DAPI (10 μg/ml). Annexin V and terminal deoxynucleotidyl transferase-mediated deoxyuridine triphosphate nick-end labeling (TUNEL) stainings were carried out using Annexin V-EGFP Apoptosis Detection Kit (MBL, Nagoya, Japan) and ApopTag Fluorescein *In situ* Apoptosis Detection Kit (Serologicals Corp., Norcross, GA, USA), respectively, according to the manufacturer's instructions. The fluorescence was observed under a Fluoview confocal laser microscope (Olympus, Tokyo, Japan). For clonogenic assay, cells were seeded at a concentration of 100 cells/well of six-well plates (Falcon 3046), incubated for 3 or 4 days under hypoxic (~0.1% O_2) conditions, and then allowed to grow under normoxic conditions for 8–10 days. Colonies were fixed with methanol and stained with 0.05% crystal violet.

Expression profiling of apoptosis-related genes
Expressions of apoptosis-related genes in normoxic and hypoxic P29 and A11 cells were carried out using Mouse Apoptosis GEArray Q™ series containing a panel of 96 key genes involved in apoptosis (SuperArray, Inc., Bethesda, MD, USA). Hybridization of the microarray with a biotin-16-dUTP-labeled cDNA probe and chemiluminescent detection were performed according to the manufacturer's instructions.

Northern blot analysis
Total RNA was electrophoresed on 1% agarose gel containing formaldehyde and transferred to nylon filters. Blots were hybridized with a ^{32}P-labeled mouse *Bnip3* cDNA probe that was prepared by RT–PCR.

Small interfering RNA (siRNA) transfection
Mcl-1 siRNA (Santa Cruz Biotechnologies, Inc., Santa Cruz, CA, USA) or Silencer Negative Control #1 siRNA (Ambion, Inc., Austin, TX, USA) was transfected into A11 cells with Lipofectamine 2000 (Invitrogen, Carlsbad, CA, USA) according to the manufacturer's protocol. At 3 days after transfection, the cells were subjected to immunoblot analysis for Mcl-1 expression, apoptosis assay and metastasis assay.

Immunoblot analysis
Cells were lysed in 1% Triton X-100, 1% sodium deoxycholate, 0.1% SDS, 50 mM Tris-HCl, pH 7.5, 150 mM NaCl, 1 mM PMSF and protease inhibitor cocktail (Sigma-Aldrich) or directly dissolved in SDS sample buffer. After centrifugation at 10 000 *g* for 10 min at 4°C, the supernatant was used for immunoblot analysis. Proteins were separated by SDS–PAGE under reducing conditions and transferred to a nitrocellulose membrane. The membrane was incubated with first antibodies, washed extensively with TBS-T, and then with species-appropriate HRP-conjugated secondary antibodies. The first antibodies used were anti-p53 antibody (Ab-3, Calbiochem-Novabiochem, Germany), anti-Mcl-1 antibody (Santa Cruz Biotechnology, Inc.), anti-GADD153 antibody (Santa Cruz Biotechnology, Inc.), anti-GRP78 antibody (Santa Cruz Biotechnology, Inc.), anti-ORP180 antibody (IBL, Fujioka, Japan) and anti-β-actin antibody (Sigma-Aldrich). Immunodetection was performed using the enhanced chemiluminescence system (ECL; Amersham Biosciences Corp., Piscataway, NJ, USA). The image of the bands was acquired with an imaging densitometer, and the signal intensities were analyzed with an NIH Image 1.63 software on a Machintosh computer. All signals were normalized to β-actin.

Tumor growth and metastasis assays
Cells (2×10^5 cells/mouse) were inoculated into the abdominal flank of age-matched female C57BL/6 mice (Nippon SLC, Hamamatsu, Japan). Subcutaneous tumor growth was monitored by caliper measurement of two diameters at right angles, and the tumor mass was estimated from the equation volume $= 0.5 \times a \times b^2$, where a and b are the larger and smaller diameters, respectively. For spontaneous metastasis assay, the mice were killed 30 days after tumor cell inoculation, and their lungs were removed. For experimental metastasis assay, tumor cells (2×10^5 cells/mouse) were injected intravenously, and the lungs were removed 17 days later. The lungs were fixed in Bouin's solution and the parietal metastatic nodules were counted. All animal experiments were performed in compliance with the institutional guidelines for the care and use of laboratory animals.

Immunohistochemistry
Subcutaneous tumors were excised, fixed in 10% buffered formalin and embedded in paraffin wax. Paraffin sections were cut at 6 μm thickness and mounted on the silane-coated glass slides. After routine dewaxing and rehydrating, the sections were incubated in 1 × ChemMate®Target Retrieval Solution (DakoCytomation, Glostrup, Denmark) at 121°C for 15 min and rinsed with Dulbecco's phosphate-buffered saline (DPBS). For quenching endogenous peroxidase activity, the sections were incubated in 0.3% H_2O_2 in methanol for 30 min. Thereafter, they were incubated with diluted normal goat serum for 20 min at room temperature and then incubated with anti-Mcl-1 antibody or normal rabbit IgG (4 μg/ml) diluted in ChemMate® Antibody Diluent (DaKoCytomation) containing 2% dry milk at 4°C for 16 h. Immunostaining was carried out by using VECTASTAIN® ABC Kit according to the

manufacturer's instructions. The sections were washed with DPBS and finally counterstained with hematoxylin.

Detection and microdissection of hypoxic areas in tumors
In all, 300 μl of EF5 solution (3 mg/ml) was injected intraperitoneally into mice bearing subcutaneous tumors (Inbal *et al.*, 1997). After 1 h, tumors were surgically removed and frozen in OCT compound. Cryostat sections cut at 10 μm were fixed with 4% paraformaldehyde and washed with DPBS. The sections were treated with 5% mouse serum, 20% dry milk and 0.3% Tween 20 in DPBS overnight at 4°C to block nonspecific binding sites. They were rinsed with 0.3% Tween 20 in DPBS and then incubated with Cy3-labeled monoclonal anti-EF5 antibody (ELK3-51) for 4 h at 4°C. After extensive washing with DPBS, tissue samples were observed under a confocal laser microscope or a fluorescence microscope. For detection of apoptotic cells *in vivo*, TUNEL staining was performed followed by EF5 staining. In some experiments, EF5 binding-positive (hypoxic) and adjacent EF5 binding-negative (normoxic) areas in tumor tissues were dissected using a laser-assisted microdissection system (Leica Microsystems, Tokyo, Japan).

Establishment of cells transfected with pEGFP-N1 or pIRES2-EGFP plasmid
P29 and A11 cells were transfected with pEGFP-N1 and pIRES2-EGFP (BD Biosciences Clontech, Tokyo, Japan), respectively, using Lipofectin reagent (Invitrogen, Tokyo, Japan). After selecting the transfected P29 or A11 cells in the presence of 800 μg/ml G418, a clone designated $P29^{EGFP}$ or $A11^{IRES\text{-}EGFP}$, respectively, was established. They were routinely cultured in the presence of 400 μg/ml G418.

DNA isolation, PCR and Southern blotting
Genomic DNA was extracted from $P29^{EGFP}$, $A11^{IRES\text{-}EGFP}$, mixed cells, solid tumors or microdissected sections by conventional method, treated with RNase A (10 μg/ml) and phenol extracted again. PCR was performed using 1–100 ng genomic DNA and *r*Taq DNA polymerase (TOYOBO Biochemicals, Osaka, Japan) on a Perkin Elmer GeneAmp PCR System 9700. The sense primer (P1) was 5′-AAC TCCGCCCCATTGACGC-3′ corresponding to the sequence within the CMV promoter, and the antisense primer (P2) was 5′-ACAAACCACAACTAGAATGCAG-3′ corresponding to the sequence in the SV40polyA signal. These primers were designed to amplify the EGFP sequence in pEGFP-N1 plasmid and the IRES-EGFP sequence in pIRES2-EGFP plasmid, thus yielding 1118 and 1693 bp PCR products, respectively. The PCR conditions were 94°C for 3 min, followed by 20–30 cycles of 94°C for 30 s, 55°C for 30 s and 72°C for 1 min. The resulting PCR products were electrophoresed on 1.2% agarose gels, transferred to nylon membranes and hybridized with a ^{32}P-labeled *EGFP* cDNA. The membranes were washed and radioactive intensity corresponding to the EGFP and IRES-EGFP bands was quantitated using a Fluoro Image Analyzer FLA-5000 (FUJIFILM, Tokyo, Japan). The measured percentage of $A11^{IRES\text{-}EGFP}$ cells was determined by dividing the intensity of the IRES-EGFP band by the total intensity of the EGFP plus IRES-EGFP bands. The actual percentage of $A11^{IRES\text{-}EGFP}$ cells in a mixed culture and in a tumor was determined from a standard curve established from Figure 6f.

Acknowledgements
We thank the National Cancer Institute (CTEP) for providing EF5. This work was supported in part by Grant-in-Aid from the Ministry of Health, Labour, and Welfare for Third Term Comprehensive Control Research for Cancer and from the Ministry of Education, Culture, Sports, Science and Technology.

References

Brizel DM, Scully SP, Harrelson JM, Layfield LJ, Bean JM, Prosnitz LR *et al.* (1996). *Cancer Res* **56**: 941–943.
Brizel DM, Sibley GS, Prosnitz LR, Scher RL, Dewhirst MW. (1997). *Int J Radiat Oncol Biol Phys* **38**: 285–289.
Brown JM, Giaccia AJ. (1998). *Cancer Res* **58**: 1408–1416.
Bruick RK. (2000). *Proc Natl Acad Sci USA* **97**: 9082–9087.
Bufalo DD, Biroccio A, Leonetti C, Zupi G. (1997). *FASEB J* **11**: 947–953.
Cairns RA, Kalliomaki T, Hill RP. (2001). *Cancer Res* **61**: 8903–8908.
Chaplin DJ, Hill SA. (1995). *Br J Cancer* **71**: 1210–1213.
Coquelle A, Toledo F, Stern S, Bieth A, Debatisse M. (1998). *Mol Cell* **2**: 259–265.
Dachs GU, Chaplin DJ. (1998). *Semin Radiat Oncol* **8**: 208–216.
Durand RE, Sham E. (1998). *Int J Radiat Oncol Biol Phys* **42**: 711–715.
Fernandez Y, Espana L, Manas S, Fabra A, Sierra A. (2000). *Cell Death Differ* **7**: 350–359.
Friedman AD. (1996). *Cancer Res* **56**: 3250–3256.
Glinsky GV. (1997). *Crit Rev Oncol Hematol* **25**: 175–186.
Glinsky GV, Glinsky VV. (1996). *Cancer Lett* **101**: 43–51.
Graeber TG, Osmanian C, Jacks T, Housman DE, Koch CJ, Lowe SW *et al.* (1996). *Nature* **379**: 88–91.
Graham CH, Forsdike J, Fitzgerald CJ, Macdonald-Goodfellow S. (1999). *Int J Cancer* **80**: 617–623.
Guo K, Searfoss G, Krolikowski D, Pagnoni M, Franks C, Clark K *et al.* (2001). *Cell Death Differ* **8**: 367–376.
Harris AL. (2002). *Nat Rev* **2**: 38–47.
Hill RP. (1990). *Cancer Metastasis Rev* **9**: 137–147.
Höckel M, Schlenger K, Aral B, Mitze M, Schaffer U, Vaupel P. (1996). *Cancer Res* **56**: 4509–4515.
Höckel M, Schlenger K, Höckel S, Vaupel P. (1999). *Cancer Res* **59**: 4525–4528.
Inbal B, Cohen O, Polak-Charcon S, Kopolovic J, Vadai E, Eisenbach L *et al.* (1997). *Nature* **390**: 180–184.
Kim CY, Tsai MH, Osmanian C, Graeber TG, Lee JE, Giffard RG *et al.* (1997). *Cancer Res* **57**: 4200–4204.
Kinoshita M, Johnson DL, Shatney CH, Lee YL, Mochizuki H. (2001). *Int J Cancer* **91**: 322–326.
Koshikawa N, Iyozumi A, Gassmann M, Takenaga K. (2003). *Oncogene* **22**: 6717–6724.
Kuwabara K, Matsumoto M, Ikeda J, Hori O, Ogawa S, Maeda Y *et al.* (1996). *J Biol Chem* **271**: 5025–5032.
Lord EM, Harwell L, Koch CJ. (1993). *Cancer Res* **53**: 5721–5726.
Lowe SW, Lin AW. (2000). *Carcinogenesis* **21**: 485–495.
Maeta Y, Tsujitani S, Matsumoto S, Yamaguchi K, Tatebe S, Kondo A *et al.* (2004). *Gastric Cancer* **7**: 78–84.
McConkey DJ, Greene G, Pettaway CA. (1996). *Cancer Res* **56**: 5594–5599.
Munro S, Pelham HR. (1986). *Cell* **46**: 291–300.

Piret JP, Minet E, Cosse JP, Ninane N, Debacq C, Raes M *et al.* (2005). *J Biol Chem* **280**: 9336–9344.
Ray R, Chen G, Vande Velde C, Cizeau J, Park JH, Reed JC *et al.* (2000). *J Biol Chem* **275**: 1439–1448.
Rice GC, Hoy C, Schimke RT. (1986). *Proc Natl Acad Sci USA* **83**: 5978–5982.
Russo CA, Weber TK, Volpe CM, Stoler DL, Petrelli NJ, Rodriguez-Bigas M *et al.* (1995). *Cancer Res* **55**: 1122–1128.
Semenza GL. (2000). *Crit Rev Biochem Mol Biol* **35**: 71–103.
Semenza GL. (2002). *Trends Mol Med* **8**: S62–S67.
Shtivelman E. (1997). *Oncogene* **14**: 2167–2173.
Takaoka A, Adachi M, Okuda H, Sato S, Yawata A, Hinoda Y *et al.* (1997). *Oncogene* **14**: 2871–2977.
Takasu M, Tada Y, Wang JO, Tagawa M, Takenaga K. (1999). *Clin Exp Metastasis* **17**: 409–416.
Teicher BA. (1994). *Cancer Metastasis Rev* **13**: 139–168.
Vande Velde C, Cizeau J, Dubik D, Alimonti J, Brown T, Israels S *et al.* (2000). *Mol Cell Biol* **20**: 5454–5468.
Wong CW, Lee A, Shientag L, Yu J, Dong Y, Kao G *et al.* (2001). *Cancer Res* **61**: 333–338.
Young SD, Hill RP. (1990). *J Natl Cancer Inst* **82**: 371–380.

Cell

Control of Developmental Regulators by Polycomb in Human Embryonic Stem Cells

Tong Ihn Lee,[1,8] Richard G. Jenner,[1,8] Laurie A. Boyer,[1,8] Matthew G. Guenther,[1,8] Stuart S. Levine,[1,8] Roshan M. Kumar,[1] Brett Chevalier,[1] Sarah E. Johnstone,[1,2] Megan F. Cole,[1,2] Kyo-ichi Isono,[3] Haruhiko Koseki,[3] Takuya Fuchikami,[4] Kuniya Abe,[4] Heather L. Murray,[1] Jacob P. Zucker,[6] Bingbing Yuan,[1] George W. Bell,[1] Elizabeth Herbolsheimer,[1] Nancy M. Hannett,[1] Kaiming Sun,[1] Duncan T. Odom,[1] Arie P. Otte,[5] Thomas L. Volkert,[1] David P. Bartel,[1,2] Douglas A. Melton,[6] David K. Gifford,[1,7] Rudolf Jaenisch,[1,2] and Richard A. Young[1,2,*]

[1]Whitehead Institute for Biomedical Research, 9 Cambridge Center, Cambridge, MA 02142, USA

[2]Department of Biology, Massachusetts Institute of Technology, Cambridge, MA 02139, USA

[3]Developmental Genetics Group, RIKEN Center for Allergy and Immunology, 1-7-22, Suehiro, Tsurumi-ku, Yokohama, Kanagawa 230-0045, Japan

[4]Technology and Development Team for Mammalian Cellular Dynamics, BioResource Center, RIKEN Tsukuba Institute, 3-1-1, Koyadai, Tsukuba, Ibaraki 230-0045, Japan

[5]Swammerdam Institute for Life Sciences, University of Amsterdam, 1098 SM Amsterdam, The Netherlands

[6]Howard Hughes Medical Institute, Department of Molecular and Cellular Biology, Harvard University, Cambridge, MA 02138, USA

[7]MIT CSAIL, 32 Vassar Street, Cambridge, MA 02139, USA

[8]These authors contributed equally to this work.

*Contact: young@wi.mit.edu

DOI 10.1016/j.cell.2006.02.043

SUMMARY

Polycomb group proteins are essential for early development in metazoans, but their contributions to human development are not well understood. We have mapped the Polycomb Repressive Complex 2 (PRC2) subunit SUZ12 across the entire nonrepeat portion of the genome in human embryonic stem (ES) cells. We found that SUZ12 is distributed across large portions of over two hundred genes encoding key developmental regulators. These genes are occupied by nucleosomes trimethylated at histone H3K27, are transcriptionally repressed, and contain some of the most highly conserved noncoding elements in the genome. We found that PRC2 target genes are preferentially activated during ES cell differentiation and that the ES cell regulators OCT4, SOX2, and NANOG cooccupy a significant subset of these genes. These results indicate that PRC2 occupies a special set of developmental genes in ES cells that must be repressed to maintain pluripotency and that are poised for activation during ES cell differentiation.

INTRODUCTION

Embryonic stem (ES) cells are a unique self-renewing cell type that can give rise to the ectodermal, endodermal, and mesodermal germ layers during embryogenesis. Human ES cells, which can be propagated in culture in an undifferentiated state but selectively induced to differentiate into many specialized cell types, are thought to hold great promise for regenerative medicine (Thomson et al., 1998; Reubinoff et al., 2000; Mayhall et al., 2004; Pera and Trounson, 2004). The gene expression program of ES cells must allow these cells to maintain a pluripotent state but also allow for differentiation into more specialized states when signaled to do so. Learning how this is accomplished may be key to realizing the therapeutic potential of ES cells and further understanding early development.

Among regulators of development, the Polycomb group proteins (PcG) are of special interest. These regulators were first described in *Drosophila*, where they repress the homeotic genes controlling segment identity in the developing embryo (Lewis, 1978; Denell and Frederick, 1983; Simon et al., 1992; Orlando and Paro, 1995; Pirrotta, 1998; Kennison, 2004). The initial repression of these genes is carried out by DNA binding transcriptional repressors, and PcG proteins modify chromatin to maintain these genes in a repressed state (Duncan, 1986; Bender et al., 1987; Strutt et al., 1997; Horard et al., 2000; Hodgson et al., 2001; Mulholland et al., 2003).

The PcG proteins form multiple Polycomb Repressive Complexes (PRCs), the components of which are conserved from *Drosophila* to humans (Franke et al., 1992; Shao et al., 1999; Birve et al., 2001; Tie et al., 2001; Cao et al., 2002; Czermin et al., 2002; Kuzmichev et al., 2002; Levine et al., 2002). The PRCs are brought to the site of initial repression and act through epigenetic modification of chromatin structure to promote gene silencing (Pirrotta,